PHYSICAL REVIEW A VOLUME 15, NUMBER 4 APRIL 1977

Origin of intermittency in fully developed turbulence

Eric D. Siggia
*Department of Physics, University of Pennsylvania, Philadelphia, Pennsylvania 19174**
and IBM Thomas J. Watson Research Center, Yorktown Height, New York 10598
(Received 5 August 1976)

Qualitative arguments based on the physics of vortex stretching indicate that Kolmogorov's mean-field theory of strong turbulence must be unstable and tend to a state in which fluctuations become increasingly singular at short distances, as proposed by Kolmogorov and Oboukhov in 1962. The number of coupled degrees of freedom in the Navier-Stokes equations is then greatly reduced by a wave-packet analysis, and the essence of the vortex stretching picture is recovered. Numerical integration of the reduced equations confirms the qualitative arguments for intermittency and gives exponents and probability distributions in crude agreement with experiment and the log-normality hypothesis.

I. INTRODUCTION

Paul Martin noted some time ago that in a number of respects the difficulties that stand in the way of a quantitative understanding of fully developed turbulence are already present in the theory of second-order phase transitions.[1-3] Both problems involve many coupled degrees of freedom and exhibit nontrivial universal scaling behavior. While our approach was motivated in a general way by Wilson's highly successful theory of second-order phase transitions, we do not make use of analogies. Instead, we attempt a semiquantitative solution of the fluid equations which seems to illustrate many of the phenomena seen experimentally. We base our approximations, insofar as possible, on the physics of turbulent flow.

A fundamental problem in turbulence theory, beyond the nonlinearity of the equations, is the necessity of dealing with a system that is not in thermal equilibrium. It is generally believed possible to establish a stationary turbulent state by continuously driving the system; but there is no simple way to determine the corresponding probability distribution. We will assume that the Navier-Stokes equations of fluid mechanics are an adequate description of a simple incompressible turbulent fluid.[2] Although they are first order in time, their laminar solutions for parameters appropriate to a strongly turbulent system are generally unstable and give rise to the chaotic nondeterministic motions characteristic of turbulence.[2] It is the statistical mechanics of these motions we wish to study.

A phenomenological theory proposed by Kolmogorov and others 35 years ago still constitutes the basis of our understanding of homogeneous fully developed turbulence.[2] It utilizes only the conservation properties of the Navier-Stokes equations and some qualitative aspects of the mechanism of energy degradation in three dimensions. Kolmogorov proposed that there exists a stationary turbulent state in which energy is transferred at a constant rate from large distances, characteristic of the driving force, to shorter distances where it is dissipated. An essential feature of this process in three dimensions is its locality in Fourier space. This means that on a logarithmic scale, the energy entering a given decade or shell of wave numbers comes predominately from the preceding decade. The fractional contribution from the earlier decades decreases exponentially. The Kolmogorov theory is summarized in Sec. II. Section III contains a simplified model of the energy transfer process and a demonstration that the so called cascade is local. It also makes plausible the direction of energy transfer in three dimensions.

Kolmogorov's theory works quite well for the energy spectrum but fails badly when applied to the fluctuations in the local dissipation rate.[4-7] Experiments suggest, but do not measure directly, that the energy transfer from shell to shell is not steady but intermittent; exhibiting strong short bursts with longer periods of quiescence. A number of phenomenological pictures of intermittency exist, although none makes any detailed use of the Navier-Stokes equations.[4, 7, 8]

A dynamical mechanism for intermittency is proposed in this paper and tested on an approximation to the Navier-Stokes equations. Physical arguments are given for why small fluctuations about Kolmogorov's stationary state amplify—become greater in magnitude but sharper in time—as they cascade to shorter distances. The locality of the energy transfer process in effect permits one to build up rather singular behavior by a sequence of more or less regular steps.

Our calculation is done on a set of equations that span a range of 2^4 in wave number and include four cascade steps. Energy was added at small k and

removed at large k in a self-consistent fashion. The equations are derived by a wave-packet decomposition of the Navier-Stokes equations. The wave packets are a compromise between Fourier space and real space. They manifest the locality in wave number of the energy cascade as well as some degree of locality in real space, which essentially means that distant eddies of the same characteristic size don't interact. After various approximations, the number of modes we have to retain increases only as the logarithm of the wave-number range spanned rather than the cube as in a direct simulation. The equations for the time dependence of the amplitudes of the wave packets are nonlinear and have the same conservation laws and symmetries as the Navier-Stokes equations.

When our equations are integrated numerically, they are stable in spite of large fluctuations and correlation functions approximately scale with wave number. Several exponents that measure the intermittency corrections to Kolmogorov's theory are in semiquantitative accord with experiment. Our results do not constitute a systematic theory of strong turbulence since our approximations are only physically plausible rather than being an expansion in some small parameter.

Section IV contains the wave-packet analysis of the Navier-Stokes equations and Sec. V our numerical results. In the conclusion we summarize those of our results which are new, consider their limitations, and relate them to earlier work.

II. MEAN-FIELD THEORY

Kolmogorov's phenomenological theory of strong turbulence is commonly presented as an application of naive dimensional reasoning.[2] The energy spectrum he found has abundant experimental support,[7] and the concept of an energy cascade is central to what follows. In short, Kolmogorov's theory stands in the same relation to fully developed turbulence that mean-field theory does to a second-order phase transition. This section contains the equations for a simple fluid and a demonstration that Kolmogorov's theory is a solution to them that neglects fluctuations. A number of additional assumptions will become apparent and a number of useful concepts and notations introduced.

The Fourier transformed Navier-Stokes equations for an incompressible fluid may be written as[2]

$$\frac{\partial}{\partial t} V^{\alpha}(\vec{k},t)+i\sum_{\beta}(\delta^{\alpha\beta}-k^{\alpha}k^{\beta}/k^2)\int \vec{V}(\vec{k}-\vec{q},t)\cdot\vec{q}\,V^{\beta}(\vec{q},t)\frac{d^3q}{(2\pi)^3}+\frac{k^2}{R}V^{\alpha}(\vec{k},t)=0,\quad \vec{k}\cdot\vec{V}(\vec{k},t)=0. \tag{2.1}$$

The density is taken as unity, and the pressure has been eliminated by subtracting out the longitudinal component of the convection term, $\vec{V}\cdot\nabla\vec{V}$. It will be a consequence of Kolmogorov's theory, that neither the boundary conditions nor the shape of the container implicit in a Fourier transform matter for the local properties of fully developed turbulence. The units of length and time are L, the dimension of the container transverse to the direction of maximum shear, and L/u where u is the variation of the velocity over distances $\sim L$. The only fluid-dependent number in Eq. (2.1) is the kinematic viscosity ν, that multiplied the last term, and was replaced by the dimensionless Reynolds number, $R=uL/\nu$. Fully developed turbulence is the limiting behavior of Eq. (2.1) as $R\to\infty$.

One might expect that the dissipative term would be negligible if R is large and the wave number is less than a cutoff Λ_K. In the inertial range, $1\ll k\ll\Lambda_K$, the equations are strongly nonlinear although the energy, $\frac{1}{2}\int_0^{\infty}\vec{V}_k\cdot\vec{V}_{-k}\,d^3k/(2\pi)^3$, is conserved. Beyond Λ_K, the convective term is a perturbation on a basically linear dissipative equation. Imagine a shearing motion that adds energy to the system at $k\sim 1$. Then, due to the nonlinear term, there will be a tendency toward equipartition as the energy spreads to higher wave numbers.[9] The energy cascade operates until $k\sim\Lambda_K$.

With these concepts, Kolmogorov's assumptions for isotropic turbulence can be stated: (i) Neglect fluctuations, i.e., replace the velocity by its root mean square. (ii) The cascade is local in wave number. (iii) Energy is transferred from large spatial scales to small ones.

Averages may be taken term by term, according to (i), and therefore there exists a single characteristic length and time. The second and third assumptions imply that eddies tend to break in half or that the energy contained in scales $\sim\lambda$ is passed to eddies of size $\sim\lambda/2$ and then to $\sim\lambda/4$, etc. The cascade occurs by a series of statistically similar steps governed by the convective coupling. Clearly, the probability that $q\to p+k$ is the same as $bq\to bp+bk$ provided all wave numbers are in the inertial range.

To estimate orders of magnitude, the inertial range is usefully partitioned into wave number shells labeled by an integer n between 1 and $\sim\ln_b\Lambda_K$. The nth shell contains all wave numbers between b^n and b^{n+1} where b is a parameter ~ 2. The energy in a shell is

$$E_n = \frac{1}{2}\int_{b^n}^{b^{n+1}} \vec{V}_p \cdot \vec{V}_{-p} \frac{d^3p}{(2\pi)^3} .$$

If a stationary cascade can be realized, energy enters the nth shell at the same rate it leaves it, neglecting fluctuations. The energy lost by n is passed to $n+1$, (locality), and a parameter ϵ, independent of wave number, may be defined as the energy input to any inertial range shell. The dissipation rate ϵ is determined locally and can be estimated by rewriting Eq. (2.1) for E_n. Neglecting numerical factors,

$$\epsilon \sim b^n E_n^{3/2}$$

or

$$E_n \sim \epsilon^{2/3} b^{-2n/3} . \tag{2.2}$$

Equation (2.2) represents the energy contained in eddies of size $\sim b^{-n}$; its derivative gives Kolmogorov's "$\frac{5}{3}$ law" for the energy/wave number. The ratio of ϵ and E_n is the rate of energy turnover in a shell or eddy damping,

$$\eta_n = \epsilon^{1/3} b^{2n/3} . \tag{2.3}$$

The small eddies act kinematically like an augmented viscosity, η_n/k^2, on the larger eddies, although the energy transfer in the inertial range is conservative. Within mean-field theory, η_n is the characteristic frequency for any process on a scale $\sim b^{-n}$.

Equations (2.2) and (2.3) have several important consequences. They state that most of the energy in the fluid is contained in large scales while the small scales equilibrate most rapidly. One expects there to exist a universal quasistationary distribution for the small scales even if the system is not continuously driven. The small scales will turn over many times before the large scales have lost much energy. Details of the energy-containing modes enter only through ϵ. The cutoff Λ_K is the wave number at which the eddy damping equals the viscous loss rate k^2/R;

$$\Lambda_K \sim R^{3/4} . \tag{2.4}$$

An inertial range should exist for sufficiently large R.

III. SIMPLE MODEL OF ENERGY TRANSFER

The Kolmogorov theory is generally derived with only passing reference to the three-dimensional Navier-Stokes equations, but is known not to hold in lower (integer) dimensionality.[10] In the previous section, we attempted to make explicit the nontrivial assumptions about high Reynolds number solutions to the Navier-Stokes equations on which the Kolmogorov theory depends. The locality and direction of the energy cascade may both to a large extent be understood by an analytical calculation on a linear but three-dimensional model. The model illustrates the mechanism of energy transport in three dimensions, vortex stretching, which appears essential for any realistic treatment of the energy cascade.[10-12] The necessity of working in locally comoving or partially Lagrangian coordinates will become apparent.

Consider a large-scale $\sim Q^{-1}$ (small wave number), static irrotational flow $\vec{V}(\vec{x})$ at high Reynolds number. If at $t=0$ a small amplitude disturbance is created having wave numbers k with $\Lambda_K >> k >> Q$ and confined to a region Ω of characteristic size Λ_Ω, much smaller than Q^{-1}, what will be its subsequent behavior? It is convenient to rewrite the Navier-Stokes equations for the vorticity $\vec{\omega}$ of the disturbance. The correlation functions of $\vec{v}$ and $\vec{\omega}$ are simply related. If $|\vec{\omega}| << Q[V(Q^{-1}) - V(0)]$, one can linearize in $\vec{\omega}$;

$$\frac{\partial \vec{\omega}}{\partial t} + \vec{V} \cdot \nabla \vec{\omega} = \vec{\omega} \cdot \nabla \vec{V} . \tag{3.1}$$

By assumption, $\vec{V}(\vec{x})$ is slowly varying over Ω and may be expanded in a Taylor series about the center of Ω.

$$\vec{V}(x) = \vec{V}(0) + \vec{\lambda} \cdot \vec{x} + \cdots . \tag{3.2}$$

Higher-order terms are a factor $Q\Lambda_\Omega$ smaller than those retained. Since Coriolis forces were neglected ($\nabla \times \vec{V} = 0$), the matrix λ is symmetric and traceless ($\nabla \cdot \vec{V} = 0$). In a coordinate system that diagonalizes λ,

$$V^\alpha(\vec{x}) = V^\alpha(0) + \lambda^\alpha x^\alpha . \tag{3.3}$$

The first term in Eq. (3.3) is eliminated from Eq. (3.1) by the substitution $\vec{x} \to \vec{x} - \vec{V}(0)t$. It is only the shear, λ, that is responsible for the growth or decay of $\vec{\omega}$. Equation (3.1) assumes the form of a differential scale transformation and may be solved in terms of the initial value of ω^α, ($\alpha, \beta = 1, 2, 3$);

$$\omega^\alpha\{x_\beta, t\} = e^{\lambda_\alpha t} \omega_0^\alpha (e^{-\lambda_\beta t} x_\beta).$$

The energy is most easily calculated from $\langle \vec{v}_k \cdot \vec{v}_{-k} \rangle = \langle \vec{\omega}_k \cdot \vec{\omega}_{-k} \rangle / k^2$:

$$E(t) = \frac{1}{2} \sum_\alpha e^{2\lambda_\alpha t} \int_\Omega d^3x \, \langle \omega_0^\alpha \omega_0^\alpha \rangle (\vec{x}) \left(\sum_\beta x_\beta^2 e^{2\lambda_\beta t} \right)^{-1/2} .$$

The temporal development of the region Ω in which $\vec{\omega} \neq 0$ is easily visualized because the shearing force acts like a volume-preserving ($\mathrm{tr}\lambda = 0$) scale transformation. If $\lambda_x, \lambda_y < 0$ and $\lambda_z > 0$, Ω becomes pencil shaped while if $\lambda_z < 0$ and $\lambda_x, \lambda_y > 0$, Ω becomes pancake shaped.

The temporal behavior of the energy depends on the initial conditions and λ_α in a detailed way.

Only several limiting cases have been investigated, but they seem to give a consistent picture of the physics. If the vorticity is initially nonzero in all three directions, let λ_m be largest λ_α and E_m the corresponding energy. There is a trivial lower bound:

$$E(t) \geq e^{\lambda_m t} E_m(0).$$

At sufficiently long times, the energy will exceed its initial value. For $t(\sum_\alpha \lambda_\alpha^2)^{1/2} \ll 1$, and an initially isotropic vorticity distribution, the energy becomes

$$E(t) = E(0)\left[1 + \frac{8}{15}\left(\sum_\alpha \lambda_\alpha^2\right) t^2 + \cdots\right].$$

If $\vec{\omega}$ is initially isotropic, $\lambda_x = \lambda_y$, $\lambda_z = -2\lambda_x$, and we define $\gamma = e^{\lambda_z t}$

$$E(t) = \tfrac{1}{3}E(0)(\gamma^2 + 2\gamma^{-1}) \begin{cases} \dfrac{\sqrt{\gamma}}{(\gamma^3 - 1)^{1/2}} \ln((\gamma^3 - 1)^{1/2} + \gamma^{3/2}) & \lambda_z > 0 \\ \dfrac{\sqrt{\gamma}}{(1 - \gamma^3)^{1/2}} \sin^{-1}((1 - \gamma^3)^{1/2}) & \lambda_z < 0. \end{cases}$$

The energy increases as $\gamma \ln\gamma$ for $\lambda_z > 0$ and as $\gamma^{-1/2}$ for $\lambda_z < 0$.

From these examples, we expect that the energy of any sufficiently isotropic distribution will increase monotonically and eventually exponentially when sheared by larger scales. Recall, however, that the equations of motion are time reversal invariant. If the initial distribution of vorticity is pencil shaped and symmetric about the z axis, and $\lambda_z < 0$, $\lambda_x, \lambda_y > 0$, the energy will decrease until the distribution is spherical and only then increase.

Our simple model of vortex stretching contains two important implications for high Reynolds number flows: the energy cascade is local, provided the distribution of shell energies, E_l, is "close" to Kolmogorov's, and $\epsilon > 0$. The former was anticipated when a transformation was made to comoving coordinates in order to remove the constant term in V, Eq. (3.3). To exploit Galilean invariance, the velocity is written as a short-wavelength part v (shells $\geq n$) and a long-wavelength piece V (shells $< n$). In analogy to Eq. (3.1), the Euler equations become

$$\frac{\partial \vec{v}}{\partial t} + \vec{V}\cdot\nabla\vec{v} + \vec{v}\cdot\nabla\vec{V} + \vec{v}\cdot\nabla\vec{v} + \vec{V}\cdot\nabla\vec{V} = 0. \qquad (3.4)$$

A transverse projection operator multiplying the nonlinear terms is understood. The wave vector of $\vec{V}\cdot\nabla\vec{V}$ will only fall into shell n if both factors are in shell $n-1$; so it is already local. The first and third terms contribute to the energy current for v while the second and fourth are volume sources or sinks of energy.

The uniform part of V has no effect on the second term and may again be removed by a coordinate transformation from the first term. The meaning of "uniform" is no longer clearcut since there is now a continuum of wave numbers rather than two distant bands. The concept still applies approximately, and it remains true that only the gradient of V affects the intrinsic or internal dynamics of v.

It is now possible to give a simple estimate of the degree of locality of the energy cascade.[13] The contribution to the logarithmic derivative of the energy, $\frac{1}{2}\int v^2$, from a shell $m < n$ is $\sim b^m$ rms (V_m) or $\sim b^{2m/3}$ if the Kolmogorov value of $E_m \sim V_m^2$, (2.2), is used. The largest shear and the most important source of energy occurs when $m = n-1$. Shells $m \ll n$ act primarily as a coordinate transformation.

By intrinsic or internal dynamics is meant what is measured in locally comoving coordinates. These coordinates are a compromise between Lagrangian coordinates which track the velocity at a given fluid point and Eulerian coordinates fixed in space. The former greatly complicate the viscous terms and require a knowledge of the velocity for all wave numbers simultaneously. Eulerian coordinates are the most convenient description in the dissipative region but suffer from spurious convection effects. The Eulerian response function is dominated by the passive convection of the test perturbation past the point of observation. A mixed representation corresponds to the description of scales $\sim\lambda$ from a neutrally buoyant platform also of size $\sim\lambda$. It combines an Eulerian description of much smaller scales with the larger scales affecting primarily the origin of coordinates. The characteristic time in the nth shell is only $\sim b^{2n/3}$ in comoving coordinates. The necessity of "mixed" coordinates was recognized by the Russian school and further developed by Kraichnan.[14]

The direction of energy transfer implied by $\epsilon > 0$ is a central tenet of isotropic turbulence theories in three dimensions. Our linear model, as it stands, is time reversal invariant and could give energy transfer in either direction. It becomes relevant to turbulence when a nonlinear intrashell coupling is included [Eq. (3.4), third term] even though it is no longer exactly solvable. Because small scales turn over more frequently than the scales that drive them, they equilibrate to an isotropic distribution more rapidly than the large scales can vary. When $\vec{\omega}$ is isotropic in our example, its energy increased. The comparatively rapid equilibration among modes in the same shell is responsible for the irreversibility of the energy

transfer between large and small scales.

One reason for undertaking numerical calculations was to verify these qualitative conclusions. Such calculations are discussed below and include several terms in the Taylor series, Eq. (3.2), Coriolis forces, and the correct nonlinear terms. We find numerically that the energy transfer is almost always positive in spite of fluctuations many times larger than its mean.

IV. WAVE-PACKET ANALYSIS OF THE NAVIER-STOKES EQUATIONS

A wave-number shell l was defined in the previous section to include all wave numbers k satisfying $b^l \leq k < b^{l+1}$. In mean-field theory, the shells were simply a shorthand to facilitate estimating orders of magnitude, though Kolmogorov's theory might be viewed as a decomposition of the Navier-Stokes equations that left only two "modes" per shell, the energy and eddy damping. In this section, the Fourier modes k are reexpressed as effective eddies or wave packets, and the energy cascade is represented by only a fixed number of basis functions in each shell.[3] In these coordinates, the Navier-Stokes equations are approximately "diagonal."

It will emerge that our intershell coupling is only exact for well-separated shells, and one would question its application to equations having a local cascade. This property alone would not disqualify our approximation if b were permitted to increase. With larger shells, most modes are interior ones coupled primarily to others in the same shell, and more degrees of freedom permit a better representation of the intrashell coupling. A larger shell also picks up the tails in the energy transfer process. A fixed long-wavelength mode q contributes $q^{2/3}$ to the characteristic frequency of energy fluctuations of all the modes in a shell. There is no contradiction to our earlier estimates because the characteristic frequency increases as $k^{2/3}$ and $q^{2/3}$ becomes a smaller percentage of the former as k increases. What invalidates a large b theory, even if it were tractable numerically, is the distribution of energy within the shell. A 50% error for modes between b^l and $2b^l$ is more serious than an equivalent error for all modes between $2b^l$ and b^{l+1}. In addition, there is no guarantee that even small errors do not propagate when integrated over long times.

Although numerical calculations were done with $b=2$, it is helpful to retain a general b in the bounds that follow. The wave-packet modes are most accurately defined when b is large. Because we are able to give a fairly precise meaning to the basis functions even when $b=2$, there are no free parameters in our equations. In a sense our expansion parameter is $2^{-2/3}$, so the final measure of success or failure must be the reasonableness and consistency of the final output.

The subsequent analysis is rather lengthy and one should not lose sight of its heuristic motivation. There are both kinematic and dynamic reasons why the Navier-Stokes equations are difficult to diagonalize. The incompressibility constraint becomes $\vec{k}\cdot\vec{V}(\vec{k},t)=0$ in momentum space, or the condition that the velocity flux out of any closed surface in real space is zero. Thus for a highly convoluted surface of average dimension b^{-l}, the incompressibility condition will mix the velocity in shell l with higher shells. The extent of mixing depends on the minimum spatial scale of the irregularities, but for a given surface decreases with b^{-1}. Large-scale coherent but very thin or fine structures occupy only a small portion of phase space, that hopefully restricts their dynamical significance.[10]

The Navier-Stokes equations themselves contain a convective term local in space and a pressure term, local in wave number, that enforces incompressibility. The pressure couples locally defined basis functions, and the convective term mixes Fourier modes. The basis adopted is a compromise in which each mode occupies a limited region or "box" ($\sim b^{-3l}$ for shell l) but includes a discrete wave-number index that runs from b^l to b^{l+1} in magnitude so as to keep the total number of degrees of freedom within a shell unchanged. If b is large, surface effects can be neglected by making the discrete set of Fourier modes periodic in the box. The incompressibility condition (e.g., the pressure) is partially satisfied by the Fourier modes, while the convective term does not couple distant boxes.

More physically, a box contains a number of eddies of some characteristic size. There is interaction between eddies of different characteristic sizes occupying the same region of space, but not with eddies of the same size in distant regions. The lth box sits within boxes representing the $l-1$, $l-2,\ldots$, shells and contains a multiplicity of boxes from shells $l+1$, $l+2,\ldots$. If intrashell interactions do not significantly couple different boxes then all the b^3 $l+1$ boxes in each l box are statistically equivalent and independent. They are all driven by the same large eddy though perhaps with different phases. For a fixed configuration in a given l box, we assume that an average over the b^3 $l+1$ boxes it contains is equivalent to a time average computed for any $l+1$ box with the constraint that the l box be in the given configuration. Making similar assumptions with l replaced by $l-1$, etc., implies a time average

over any box in shell l is equal to an average over all the l boxes present at an instant of time. This conclusion we believe to be correct even when intrashell interactions are present, although we will argue in this section that retaining only one box per shell is a reasonable first approximation.

The reaction of the boxes in shell $l+1$ back on shell l can be kinematically represented by an eddy viscosity which is then chosen to conserve energy. At each instant of time the eddy viscosity should be determined by the energy entering all the b^3 $l+1$ boxes. Instead, we will retain only one box per shell and use it alone to fix the eddy viscosity. Qualitative arguments for why this last approximation could either decrease or increase the intermittency are left for the conclusion since they relate to the connection of our model to Mandelbrot's geometric description of intermittency.[8]

Our "boxes" represent a convenient decomposition of the degrees of freedom within a shell at an instant of time but should not be taken too literally. If a region in the fluid were marked off initially, its surface would immediately be rippled by the small scales, and eventually it would be pulled and stretched into a highly convoluted surface by the larger scales. It was argued at the end of the last section that a comparatively rapid equilibration takes place among the modes in a shell, that renders them isotropic and is responsible for the unidirectional energy cascade. The size of b determines the maximum degree of asymmetry or disequilibration that can be tolerated within our enumeration of the degrees of freedom. If a blob is pulled into a long thin sheet, it can no longer be described by the modes of a single box.

The decomposition of the Navier-Stokes equations into a wave-packet basis breaks up into several parts. The velocity is written as a sum of the new basis functions with time-dependent amplitudes. This representation is substituted into the Navier-Stokes equations and the various intrashell and intershell couplings identified and compared. Our intention in this section is to demonstrate why it is reasonable to consider only one box per shell and neglect its interaction with its neighbors in the same shell; in effect thinning the degrees of freedom. The limitations of our model are discussed in Sec. V and the conclusion. The actual form of the interaction between the modes in a given box and their coupling to the preceding shell for $b=2$ are reserved for Sec. V.

It has been implicitly assumed until now that the entire fluid is contained in a cube of volume $(2\pi)^3$ and that consequently wave numbers run from one to infinity. The remainder of this section focuses on a particular shell l and its immediate neighbors in the inertial range. It is convenient to use new units in which the fluid occupies a cube $2\pi b^l$ on a side and the lth shell contains wave numbers between 1 and b.

The following notation is used consistently:

$\vec{H}$, $\vec{G}$, $\vec{F}$ label the discrete Fourier modes in the boxes for shells $l-1$, l, $l+1$ (when several shells figure in the same expression, $\vec{H}$ corresponds to $l-1$, etc.). Their components take on all integer values subject to the constraint on their magnitudes $1 \leq H, G, F < b$;

$\vec{k}$ and $\vec{q}$ are continuous wave numbers between 0 (actually b^{-l}) and infinity in magnitude;

$\vec{R}_n$ runs over a lattice of points $2\pi(n^1, n^2, n^3)$, where n^i are integers, the boxes representing shell $l-1$, $(l+1)$, are centered on a lattice $\vec{R}_m$ with spacing $2\pi b$, $(2\pi b^{-1})$;

$\phi(\vec{r})$ is a smooth positive function localized in a box 2π on a side and normalized according to $\int \phi^2(\vec{r}) d^3r = (2\pi)^3$, $\vec{\phi}(k)$ is its Fourier transform.

The $\frac{4}{3}\pi\,(b^3-1)b^{3l}$ Fourier modes for each component of the velocity in shell l may be reexpressed by means of an equal number of complex amplitudes $\vec{A}^{\,l}_{G,n}(t) = \vec{A}^{\,l}_{-G,n}(t)^*$ according to

$$\vec{V}_l(\vec{r},t) = \sum_{G,n} \vec{A}^{\,l}_{G,n}(t) e^{i\vec{G}\cdot(\vec{r}-\vec{R}_n)} \phi(\vec{r}-\vec{R}_n). \quad (4.1a)$$

The sum extends over $\sim \frac{4}{3}\pi b^3$ vectors $\vec{G}$ and b^{3l} boxes with centers at $\vec{R}_n$. The analogous expressions for shells $l\pm1$ follow by scaling the wave vector and $\phi(\vec{r})$ to restrict the amplitudes to a box of appropriate size.

$$\vec{V}_{l\pm1}(\vec{r},t) = \sum_{G,m} \vec{A}^{\,l\pm1}_{G,m} \exp[ib^{\pm1}\vec{G}\cdot(\vec{r}-\vec{R}_m)]\,\phi(b^{\pm1}(\vec{r}-\vec{R}_m)). \quad (4.1b)$$

The new basis functions are clearly complete since they are equal in number to the Fourier modes in the appropriate shell. To the extent that $\phi(r)$ is not exactly zero outside of the box centered at the origin, wave functions in adjacent boxes are not precisely orthogonal. Similarly the variation in ϕ within a box means that the oscillatory functions assigned to the same box are not orthogonal. The effects of nonorthogonality decrease with b^{-1} and do not affect the rather crude estimates that follow.

The average mean-square amplitude, $\frac{1}{2}\sum_G \vec{A}^{\,l}_{G,n} \cdot \vec{A}^{\,l}_{-G,n}$, is the same in all boxes. For simplicity, we pick a unit of time that makes the energy/volume in a shell m equal $b^{-2(m-l)/3}$ in mean-field theory. (The dissipation rate ϵ is now a pure number.) Computing the energy/volume from Eq. (4.1) fixes the mean amplitude in an arbitrary box:

$$1 \simeq \frac{1}{2}\sum_{G} |\vec{A}^{l}_{G,n}|^2 ,$$
$$b^{\pm 2/3} \simeq \frac{1}{2}\sum_{G} |\vec{A}^{l\mp 1}_{G,m}|^2 . \tag{4.2}$$

The Fourier transforms of Eq. (4.1) are

$$\vec{V}_l(\vec{k},t) = \sum_{G,n} \vec{A}^{l}_{G,n}(t) e^{-i\vec{k}\cdot\vec{R}_n} \tilde{\phi}(\vec{k}-\vec{G}), \tag{4.3a}$$

$$\vec{V}_{l\pm 1}(\vec{k},t) = \sum_{G,m} \vec{A}^{l\pm 1}_{G,m} e^{-i\vec{k}\cdot\vec{R}_m} b^{\mp 3} \tilde{\phi}(b^{\mp 1}\vec{k}-\vec{G}). \tag{4.3b}$$

In Eq. (4.3a), $\tilde{\phi}(\vec{k}-\vec{G})$ restricts $\vec{k}$ to within one unit of $\vec{G}$. The momentum constraint on $\vec{k}$, $1 \leq k < b$, is automatically satisfied except for $G \simeq 1$. In the equation for $\vec{V}_{l-1}$, $\phi(b\vec{k}-\vec{G})$ restricts $\vec{k}$ to a distance $\sim b^{-1}$ from $b^{-1}\vec{G}$. The approximation,

$$\vec{k}\phi(\vec{k}-\vec{G}) = \vec{G}\phi(\vec{k}-\vec{G}), \tag{4.4}$$

and its analogs for shells $l \pm 1$ are used extensively. For most values of $\vec{G}$ the error is $\sim b^{-1}$ if b is large. Obviously for $G \simeq 1$, the distinction between shells is blurred, and our numerical approximations are only semiquantitative. The first consequence of Eq. (4.4) is a restatement of incompressibility:

$$\vec{G}\cdot\vec{A}_{G,n} = 0.$$

The Navier-Stokes equations are decomposed by writing the velocity as a sum over shells and multiplying out the nonlinear term. An expression for $d\vec{V}_l/dt$ is developed from all terms whose total wave number places them in the lth shell:

$$\frac{d}{dt}\vec{V}_l(\vec{k},t) = \sum_{n,G} \frac{d\vec{A}^{l}_{G,n}}{dt} e^{-i\vec{k}\cdot\vec{R}_n} \tilde{\phi}(\vec{k}-\vec{G}) \equiv \sum_{i,j} [\vec{V}_i \cdot \vec{\nabla}\vec{V}_{l-j}]^{\alpha} \tag{4.5}$$

(The time dependence of $\vec{R}_n$ was ignored because it cancels against the uniform part of $\vec{V}_{l-m}$ when the Galilean transform is made. The boxes of shell l are comoving with respect to $m < l$.) The shorthand expressions $[\vec{V}_i \cdot \nabla\vec{V}_{l-j}]^{\alpha}$ and $[\vec{V}_{l-j} \cdot \nabla\vec{V}_i]^{\alpha}$ denote the two possible terms (including the pressure) that arise from shells $l-j$ and i.

The intrashell coupling, $[\vec{V}_l \cdot \nabla\vec{V}_l]$, after some rearrangement and approximation is ($\alpha, \beta = 1, 2, 3$):

$$[\vec{V}_l \cdot \nabla\vec{V}_l]^{\alpha} = -i \sum_{\vec{G},\vec{G}',n} e^{-i\vec{k}\cdot\vec{R}_n} \tilde{\phi}(\vec{k}-\vec{G}) \left(\delta^{\alpha\beta} - \frac{G^{\alpha}G^{\beta}}{G^2}\right) \vec{G}' \cdot \vec{A}^{l}_{G-G',n} \times \left[\sum_{n'} A^{l,\beta}_{G',n'} e^{i\vec{G}'\cdot(\vec{R}_n - \vec{R}_{n'})} \int \frac{d^3q}{(2\pi)^3} \tilde{\phi}(\vec{q}-\vec{G}') e^{i(\vec{R}_n - \vec{R}_{n'})\cdot(\vec{q}-\vec{G}')}\right] . \tag{4.6}$$

The summations on n and n' are unrestricted, but $1 \leq |\vec{G}-\vec{G}'| < b$. The q integral is not just $\phi(\vec{R}_n - \vec{R}_{n'}) \simeq \delta_{n,n'}$ because its domain of integration is restricted to the intersection of

$$1 \leq q < b \text{ and } 1 \leq |\vec{k}-\vec{q}| < b.$$

Let D be the distance from G' to the nearest boundary. By shifting q, the domain of integration becomes a sphere of radius D plus an irregular piece. The integral over the former is

$$I_s = \phi(\vec{R}_n - \vec{R}_{n'}) - \frac{1}{|\vec{R}_n - \vec{R}_{n'}|} \times \mathrm{Im} \int_D^{\infty} \frac{p\,dp}{2\pi^2} \tilde{\phi}(p) e^{ip|\vec{R}_n - \vec{R}_{n'}|}.$$

If the second term is integrated by parts,

$$I_s = \phi(\vec{R}_n - \vec{R}_{n'}) - \frac{D\tilde{\phi}(D)\cos D|\vec{R}_n - \vec{R}_{n'}|}{2\pi^2 |\vec{R}_n - \vec{R}_{n'}|^2} \times [1 + O(1/|\vec{R}_n - \vec{R}_{n'}|)] . \tag{4.7}$$

In the remaining region of integration $p \geq D$. It is still possible to integrate over the direction of $\vec{p}$ and do an asymptotic expansion in $|\vec{R}_n - \vec{R}_{n'}|$. The result will be the same order of magnitude as the second term in Eq. (4.7). The bracketed term in Eq. (4.6) becomes

$$A^{l,\beta}_{G',n} + D\tilde{\phi}(D) \sum_{n' \neq n} A^{l,\beta}_{G',n'} \frac{\gamma(|\vec{R}_n - \vec{R}_{n'}|)}{|\vec{R}_n - \vec{R}_{n'}|^2} ,$$

where γ is an oscillatory function of order unity. The summation on n' is long ranged and represents some fluctuating velocity amplitude $\vec{C}_{G',n}$ that is uncorrelated with $\vec{A}^{l}_{G',n}$. (The long-ranged interaction helps in this respect.) The relative importance of $\vec{C}_{G',n}$, as measured by its average and variance,

$$\langle \vec{C}_{G',n} \rangle = 0 \quad \langle |\vec{C}_{G',n}|^2 \rangle \simeq [D\tilde{\phi}(D)]^2 \langle |\vec{A}^{l}_{G',n}|^2 \rangle$$

depends on G' through D.

To estimate the effect of neglecting $\vec{C}_{G',n}$ on the integration of Eq. (4.6), define a boundary to consist of all $\vec{G}'$ with $D \leq b^{\delta}$ and $\delta < 1$. A fraction of $b^{\delta-1}$ of the wave numbers $\vec{G}'$ fall into the boundary. Within the boundary $\langle |C|^2 \rangle$ is potentially as large as $\langle |A|^2 \rangle$, but elsewhere $\langle |C|^2 \rangle / \langle |A|^2 \rangle$ decreases with b^{-1} as some power of $b^{-\delta}$ depending on the exact shape of $\tilde{\phi}$. [Recall that $\int \tilde{\phi}(\vec{q})\, d^3q/(2\pi)^3 \sim 1$ and $\phi(\vec{r})$ has a characteristic size ~ 1.] With these estimates have to be folded the relative magnitudes

of $|A_G^2|$, that may be taken from mean-field theory. In Eq. (4.6), $A_{G-G'}$ is largest when $\vec{G}\sim\vec{G}'$. If $G\sim b$, $G'\sim 1$ may be neglected. The mean square of the remaining factor in Eq. (4.6), $G'A_{G'}$, is distributed according to $G'^{1/3}dG'$. The importance of the boundaries is reduced by b^{-6} relative to the interior, e.g., $\sim\int_{b-b^{\delta}}^{b}/\int_{\sim 1}^{b}$; the neglect of $\langle|C|^2\rangle$ introduces a similar error. If $G\sim 1$, both neglecting $\langle|C|^2\rangle$ and using Eq. (4.4) can introduce appreciable errors. The contribution to Eq. (4.5) from Eq. (4.6) finally reads,

$$\frac{dA_{G,n}^{l,\alpha}}{dt} = -i(\delta^{\alpha\beta}-G^{\alpha}G^{\beta}/G^2)\times\sum_{\vec{G}}(\vec{G}'\cdot\vec{A}^{l}_{G-G',n}A^{l,\beta}_{G',n})+\cdots,$$

subject to $1\leq|\vec{G}-\vec{G}'|<b$.

The most important terms coupling the lth shell to preceding ones are $[\vec{V}_l\cdot\nabla\vec{V}_{l-1}]$, $[\vec{V}_{l-1}\cdot\nabla\vec{V}_l]$, and $[\vec{V}_{l-1}\cdot\nabla\vec{V}_{l-1}]$. Interactions with $\vec{V}_{l-m}$ $m\geq 2$ are a factor $b^{2m/3}$ smaller (Sec. III). Equations (2.1) and (4.3) imply

$$[\vec{V}_l\cdot\nabla\vec{V}_{l-1}]^{\alpha} = -i(\delta^{\alpha\beta}-k^{\alpha}k^{\beta}/k^2)\sum_{H,G',n}e^{-i\vec{k}\cdot\vec{R}_n}\tilde{\phi}(\vec{k}-b^{-1}\vec{H}-\vec{G}')b^{-1}\vec{H}\cdot\vec{A}^{l}_{G',n}\times\sum_{m}A^{l-1,\beta}_{H,m}e^{ib^{-1}\vec{H}\cdot(\vec{R}_n-\vec{R}_m)}\int e^{i(\vec{q}-b^{-1}\vec{H})\cdot(\vec{R}_n-\vec{R}_m)}\tilde{\phi}(\vec{q}b-\vec{H})\frac{b^3d^3q}{(2\pi)^3}. \tag{4.8}$$

The $\vec{q}$ integral is restricted to $b^{-1}\leq|\vec{q}|<1$ and $1\leq|\vec{k}-\vec{q}|<b$ with $\vec{k}$ in shell l. Its value again depends on the position of $b^{-1}\vec{H}$ relative to the boundaries of the domain of integration.

The locality of the cascade, i.e., the factor $b^{-1}H$, allows consideration in Eq. (4.8) of only $H\sim b$ for b large. From this set, separate out a layer consisting of all $\vec{H}$'s within a distance $b^{1/2}$ of a boundary. This layer contributes a small fraction, $\sim b^{-4/3}\int_{b-b^{1/2}}^{b}H^{1/3}dH$, of the mean-square shear or vorticity present in box m. The remaining vectors $\vec{H}$ are at least $b^{1/2}$ from any boundary; and by scaling out the factor of b, the q integral, I, may be done in analogy to the calculation for $[\vec{V}_l\cdot\nabla\vec{V}_l]$. The spherically symmetric piece of I is

$$I_s=\phi(b^{-1}\vec{R}_n-b^{-1}\vec{R}_m)-\int_D^{\infty}e^{i\vec{p}\cdot(\vec{R}_n-\vec{R}_m)b^{-1}}\phi(\vec{p})\frac{d^3p}{(2\pi)^3}.$$

The $l-1$ boxes are spaced by $2\pi b$, and $b^{-1}\vec{R}_m$ is the same order as $\vec{R}_{n'}$ was in Eq. (4.7), and $D\geq b^{1/2}$. The second term in I_s, as well as a similar one from the irregularly shaped piece of the domain of integration, are negligible. The first term in I_s is approximately constant for the $\sim b^3$ boxes R_n contained within a given R_m. Alternately, the summation on m reduces to the single box R_m that contains a given box n.

Equation (4.8) is still not of the form of Eq. (4.5). The function $\tilde{\phi}$ restricts $\vec{k}$ to within a range ~ 1 of $b^{-1}\vec{H}+\vec{G}'$. It is apparent that the contribution to $d\vec{A}^{l}_{G,n}/dt$ will come predominantly from $\vec{G}'\sim\vec{G}$ with essentially equal weight from all values of $\vec{H}$; i.e., $b^{-1}H$ never exceeds the width of $\tilde{\phi}$. To be more precise, we expand $e^{ib^{-1}\vec{H}\cdot\vec{r}}$ in a series of $e^{i\vec{G}''\cdot\vec{r}}$,

$$\tilde{\phi}(\vec{k}-b^{-1}\vec{H}-\vec{G}')\equiv\int d^3r\,\phi(\vec{r})e^{i\vec{r}\cdot(\vec{k}-b^{-1}\vec{H}-\vec{G}')} = \sum_{\vec{G}''}\phi(\vec{k}-\vec{G}'-\vec{G}'')(-1)^{1+\Sigma_{\alpha}G''^{\alpha}}\times\prod_{\beta=1}^{3}\frac{\sin(\pi H^{\beta}b^{-1})}{\pi(G''^{\beta}-b^{-1}H^{\beta})}. \tag{4.9}$$

The contribution to Eq. (4.8) is finally

$$\frac{dA_{G,n}^{l,\alpha}}{dt} = -i(\delta^{\alpha\beta}-G^{\alpha}G^{\beta}/G^2)\sum_{G''}A^{l,\gamma}_{G-G'',n}(-1)^{1+\Sigma_{\alpha}G''^{\alpha}}\times\sum_{\vec{H}}b^{-1}H^{\gamma}A^{l-1,\beta}_{H,m}e^{ib^{-1}\vec{H}\cdot(\vec{R}_n-\vec{R}_m)}\times\prod_{\delta=1}^{3}\frac{\sin(\pi H^{\delta}b^{-1})}{\pi(G''^{\delta}-b^{-1}H^{\delta})}. \tag{4.10}$$

The sum on $\vec{G}''$ is restricted to $1\leq|\vec{G}-\vec{G}''|<b$. Some additional approximations for $b=2$ are made on Eq. (4.10) in Sec. V.

The estimate for $[\vec{V}_{l-1}\cdot\nabla\vec{V}_l]$ is similar to $[\vec{V}_l\cdot\nabla\vec{V}_{l-1}]$. The gradient now acts on $\vec{V}_l$ instead of $\vec{V}_{l-1}$ and the factor $b^{-1}\vec{H}$ in Eq. (4.8) is replaced by $\vec{G}$ or $\vec{G}'$. It might appear that small $\vec{H}$ dominate the sum. This is, of course, not true since the box at $\vec{R}_n$ has to be transformed to comoving coordinates by subtracting from $\vec{V}_{l-1}$ its integral over this box. After the Fourier expansion [Eq. (4.9)] is done, $\vec{V}_{l-1}$ is no longer exactly incompressible, and it is necessary to remove its longitudinal part if $[\vec{V}_{l-1}\cdot\nabla\vec{V}_l]$ is to contribute only to the energy current. The exact form of $[\vec{V}_{l-1}\cdot\nabla\vec{V}_l]$ is given in the next section for $b=2$.

The last coupling term $[\vec{V}_{l-1}\cdot\nabla\vec{V}_{l-1}]$, only falls within the lth shell when $k\lesssim 2$. If $b=2$ this is the

entire shell, while if b is large $[\vec{V}_{l-1}\cdot\nabla\vec{V}_{l-1}]$ affects only a small percentage of the wave vectors $\vec{G}$. Unfortunately, they contain most of the energy in the shell. This term is discussed in the following section after our model equations are written out.

To complete the equations for the lth shell requires an energy sink to represent the energy transferred to higher wave numbers. The dominant term, $[\vec{V}_{l+1}\cdot\nabla\vec{V}_{l+1}]$, stands in the same relation to $[\vec{V}_{l+1}\cdot\nabla\vec{V}_l]+[\vec{V}_l\cdot\nabla\vec{V}_{l+1}]$ (that will be neglected) as did $[\vec{V}_l\cdot\nabla\vec{V}_{l-1}]+[\vec{V}_{l-1}\cdot\nabla\vec{V}_l]$ to $[\vec{V}_{l-1}\cdot\nabla\vec{V}_{l-1}]$. The former is able kinematically to connect all wave numbers in shell $l+1$ to all those in shell l; $[\vec{V}_{l+1}\cdot\nabla\vec{V}_l]+[\vec{V}_l\cdot\nabla\vec{V}_{l+1}]$ couples only large wave numbers in shell l to small ones in $l+1$, although as before the smallest wave numbers in any shell contain most of the energy. The analogy with the two energy source terms is reinforced by calculating the energy balance. The energy transferred to the lth shell by $[\vec{V}_{l+1}\cdot\nabla\vec{V}_l]+[\vec{V}_l\cdot\nabla\vec{V}_{l+1}]$ is minus that transferred to shell $l+1$ by $[\vec{V}_l\cdot\nabla\vec{V}_l]$.

There are $\sim b^3$ boxes, $\vec{R}_m$, from shell $l+1$ that fall within each box of shell l. It is the correlations among the b^3 little boxes induced by their membership in a single large box that react back to produce an eddy damping.[15] The eddy damping is not calculated but fixed by energy conservation and approximately accounts for all damping processes.

It is easiest to estimate $[\vec{V}_{l+1}\cdot\nabla\vec{V}_{l+1}]$ in position space and anticipate that the pressure will make it transverse. The precise factors affect the eddy damping numerically but not its functional form. If Eq. (4.1b) is substituted into $[\vec{V}_{l+1}\cdot\nabla\vec{V}_{l+1}]$, and Eq. (4.5) inverted to find $\vec{A}^l_{G,n}$:

$$\frac{\partial A^{l,\alpha}_{G,n}}{\partial t}=-i\int d^3r\, e^{-i\vec{G}\cdot(\vec{r}-\vec{R}_n)}\phi(\vec{r}-\vec{R}_n)\times G^\beta\sum_{\vec{F},\vec{F}',m}A^{l+1,\beta}_{F',m}A^{l+1,\alpha}_{F,m}e^{ib(\vec{F}+\vec{F}')\cdot(\vec{r}-\vec{R}_m)}\times\phi^2(b(\vec{r}-\vec{R}_m))+\cdots.$$

The sum over $\vec{F}$ and $\vec{F}'$ is restricted to $\vec{F}=-\vec{F}'+b^{-1}\vec{G}+O(1)$ by $\phi^2(b\vec{r})$. If $G/F\ll b$, $\vec{F}=-\vec{F}'$. The $\vec{r}$ integral is trivial and restricts $\vec{R}_m$ to lie within box n:

$$\frac{\partial A^{l,\alpha}_{G,n}}{\partial t}=b^{-3}G^\beta\sum_{\vec{F},m}e^{-i\vec{G}\cdot(\vec{R}_m-\vec{R}_n)}\times A^{l+1,\beta}_{F,m}A^{l+1,\alpha}_{-F,m}+\cdots. \tag{4.11}$$

If we ignore any correlation among $\vec{A}^{l+1}_{F,m}$ the average and variance of Eq. (4.11) are $O(b^{-1})$ because the sum over $e^{-i\vec{G}\cdot\vec{R}_m}$ contributes only at the boundaries. (Remember that R_m runs over b^3 lattice points spaced by $2\pi/b$.)

The correlations that generate the eddy viscosity are found by applying Eq. (4.10) and its analogue for $[\vec{V}_{l-1}\cdot\nabla\vec{V}_l]$ to the boxes R_m in shell $l+1$. We assume $G/F\ll b$ [if $H\ll bG''$ in the notation of Eq. (4.10), the sum on $\vec{G}''$ is restricted to the neighborhood of the origin], and include an eddy viscosity.

$$\frac{\partial A^{l+1,\alpha}_{F,m}}{\partial t}+\eta_{l+1}A^{l+1,\alpha}_{F,m}=-i(\delta^{\alpha\beta}-F^\alpha F^\beta/F^2)\sum_{\vec{G}'}e^{i\vec{G}'\cdot(\vec{R}_m-\vec{R}_n)}(\vec{G}'\cdot\vec{A}^{l+1}_{F,m}A^{l,\beta}_{G',n}\gamma_1+\vec{F}\cdot\vec{A}^{l}_{G',n}A^{l+1,\beta}_{F,m}\gamma_2)+\cdots. \tag{4.12}$$

The γ's are wave-number-dependent functions. Equation (4.12) may be solved for $\vec{A}^{l+1}$ implicitly by inverting the linear terms and remembering that $\vec{A}^l$ responds more slowly than $\vec{A}^{l+1}$:

$$A^{l+1,\alpha}_{F,m}(t)=-i(\delta^{\alpha\beta}-F^\alpha F^\beta/F^2)\sum_{\vec{G}'}e^{i\vec{G}'\cdot(\vec{R}_m-\vec{R}_n)}\times\int_{-\infty}^{t}dt'\exp\left(-\int_{t'}^{t}\eta_{l+1}\right)[\vec{G}'\cdot\vec{A}^{l+1}_{F,m}(t')A^{l,\beta}_{G',n}(t)\gamma_1+\vec{F}\cdot\vec{A}^{l}_{G',n}(t)A^{l+1,\beta}_{F,m}(t')\gamma_2]+\cdots. \tag{4.13}$$

No double counting occurs if Eq. (4.13) is substituted for one of the factors of $\vec{A}^{l+1}$ in Eq. (4.11) since correlations are not relevant to the driving of small scales by large. Only the average of $\vec{A}^{l+1}\vec{A}^{l+1}$ (independent of m) contributes to the eddy damping because $\vec{V}^{l+1}$ fluctuates more rapidly than $\vec{V}^l$. The sum over m in Eq. (4.11) picks out $\vec{G}=\vec{G}'$ from Eq. (4.13) and cancels b^{-3}. The right-hand side of Eq. (4.11) after substitution of (4.13) becomes a number of order 1, the eddy damping η_l, times $A^{l,\alpha}_{G,n}$. It was necessary to assume $G\ll bF$, and approximate certain double sums by their diagonal term, because the eddy damping concept is only strictly valid when the damping modes are much smaller (and therefore faster) than the damped modes. The eddy damping is positive when energy is being transferred to progressively smaller scales.

V. RESULTS OF A LOCAL CASCADE MODEL IN EDDY COORDINATES

A simple linear model for the energy transfer process was the subject of Sec. III. In Sec. IV its essential features were recovered by a wave-packet decomposition of the Navier-Stokes equations. It is only when coupling distant bands of wave numbers that the idealized vortex-stretching mechanism and eddy-damping approximation apply quantitatively. The wave-packet variables are kinematically unambiguous only for $b \gg 2$; but the defects of the vortex-stretching idea, when applied to contiguous bands of wave numbers, are only partially remedied in this limit. Although it was only feasible computationally to work with $b = 2$, we continue to use the eddy-damping–vortex-stretching model even though several omitted terms are approximately the same magnitude as those retained. Their effects may be understood qualitatively as a perturbation of the existing model which appears to incorporate the essential physics. Only one box per shell is retained with all the boxes having the same center and orientation. The interaction among equivalent boxes was treated in the previous section.

Subsection A contains the wave-packet basis for $b = 2$, the equations for a general shell, and estimates of the order of magnitude of certain neglected terms. Their possible effects on the dynamics of the energy cascade conclude the section on fluctuations. The actual numerical integration was done on just four consecutive shells which require an energy source and sink if a stationary distribution is to result. Subsection B continues with a detailed discussion of the stability of the energy cascade, the dynamical behavior of fluctuations, and the origin of intermittency, illustrated by the time dependence of the energy and dissipation obtained numerically. It is then possible to assess the consistency of several energy sinks that could terminate a finite set of shells. Details of the numerical analysis, histograms, and a table of exponents comprise subsection C.

A. Equations for wave-packet amplitudes, $b = 2$

The smallest value of b for which a wave-packet analysis retains any meaning is $b = 2$. Equation (4.1) involved a function ϕ that localized the representation in position space yet approximately decoupled the Fourier modes in different boxes within the same shell. Surface effects, or the continuity of the velocity from box to box, are neglected by using periodic boundary conditions. Within a given box, ϕ varies less rapidly than the Fourier modes, and the numerical calculations are greatly simplified if we assume ϕ is either one or zero. For a box $(2\pi)2^{-l+1}$ on a side, we chose the 26 Fourier modes $e^{i2^{l-1}\vec{G}\cdot\vec{r}}$ for $G^\alpha = 0, \pm 1$ with wave numbers $\vec{k} = 2^{l-1}\vec{G}$ between 2^{l-1} and 2^l. Twenty-six is reasonably close to the number of modes required to preserve the density in phase space, $28\pi/3$. The velocity $\vec{V}_l(\vec{r}, t)$ is determined by 78 complex amplitudes, $\vec{A}_G^l(t)$, subject to the constraints that V_l be incompressible and real; $\vec{G}\cdot\vec{A}_G^l = 0$, $\vec{A}_G^{l*} = \vec{A}_{-G}^l$. The energy is

$$E_l = \frac{1}{2}\int_l V_l^2\, d^3r/\tau_l = \frac{1}{2}\sum_G |\vec{A}_G^l|^2 ,$$

where $\int_l$ denotes the integral over the lth box of volume $\tau_l = (4\pi 2^{-l})^3$.

The equations for an arbitrary shell are

$$\frac{\partial \vec{V}_l}{\partial t} + \vec{V}_{l-1}\cdot\nabla\vec{V}_l + \vec{V}_l\cdot\nabla\vec{V}_{l-1} + \vec{V}_l\cdot\nabla\vec{V}_l + \nabla p + (\eta_l + 2^{2l}/R)\vec{V}_l = 0 , \quad (5.1a)$$

$$2\eta_l E_l = \tau_{l+1}^{-1}\int_{l+1} V_{l+1}^\alpha\, \vec{V}_{l+1}\cdot\nabla\vec{V}_l^\alpha \equiv \epsilon_{l+1} . \quad (5.1b)$$

The second equation determines η_l from the rate energy is acquired by the following shell when the cascade is nearest neighbor.

Our reasons for omitting the $\vec{V}_{l-1}\cdot\nabla\vec{V}_{l-1}$ term in (5.1a) as a first approximation are given later in this section and again when considering intermittency. The reader should also note that this term was retained in a number of computer runs with little change in the final results.[16]

Equation (5.1) is not complete as written because V_{l-1} has twice the period of V_l and consequently the conservation properties of the first nonlinear term are not the same as in the complete Navier-Stokes equations. The intrashell coupling contributes just $\frac{1}{2}\nabla\cdot\vec{V}_l V_l^2$ to the divergence of the energy current, and the integral over box l reduces to surface terms that cancel pairwise. For $\vec{V}_{l-1}\cdot\nabla\vec{V}_l$, the analogous term is $\frac{1}{2}\nabla\cdot\vec{V}_{l-1}V_l^2$, and its integral does not vanish because V_{l-1} is not periodic in box l. To remedy this problem and extract an equation for $d\vec{A}_G^l/dt$ from Eq. (5.1), a second Fourier expansion of $\vec{V}_{l-1}$ is required [see Eq. (4.9)]. For $l = 1$, (general l found by rescaling), $\vec{V}_0$ contains wave numbers $\vec{k} = \frac{1}{2}\vec{H}$, $H^\alpha = 0, \pm 1$, while $\vec{V}_1$ is a sum of $e^{i\vec{G}\cdot\vec{r}}$. To close Eq. (5.1), expand

$$e^{i\vec{H}\cdot\vec{r}/2} = \sum_{\vec{N}} e^{i\vec{N}\cdot\vec{r}} C(\vec{N}, \vec{H}) . \quad (5.2)$$

The sum extends up to twice the maximum wave number in shell 1, because in the product $\vec{V}_{l-1}\cdot\nabla\vec{V}_l$, there will be terms like $e^{2ix}e^{-ix}$ that again fall into shell 1. The momentum constraints on shell 0 have not been violated. One could

equally well multiply out $\vec{V}_{l-1}\cdot\nabla\vec{V}_l$ and then expand each term. The procedure employed is algebraically equivalent and simpler to implement numerically.

Equation (5.2) is accurate to about 10% with the largest errors occuring near the boundaries. A function such as $\sin\frac{1}{2}x$ becomes periodic in $[-\pi,\pi]$ if expanded in e^{inx}. After Eq. (5.2) is applied to V_0, it is no longer incompressible. We project out its longitudinal part and at the same time drop its zero wave number component to effect the Galilean transformation. It was found numerically that the energy decreased by ~10% after this operation, while the energy/vol [after applying Eq. (5.2)] varies from 0.5 to 1.1 times its original value. The latter variation is believed to depend upon the spatial distribution of energy within box 0. The greatest reduction would occur when the velocity is largest near the boundaries. The contribution of $\vec{V}_0\cdot\nabla\vec{V}_1$ $(=\nabla\cdot\vec{V}_0\vec{V}_1)$ to the divergence of the energy current is still $\frac{1}{2}\nabla\cdot\vec{V}_0V_1^2$, but now reduces to surface terms that cancel pairwise when integrated over box 1. Errors in this term are not serious because it acts like $\vec{V}_1\cdot\nabla\vec{V}_1$ to redistribute the energy among the modes in box 1.

The term $\vec{V}_1\cdot\nabla\vec{V}_0$ is the only one to transfer energy from box 0 to 1. It is necessary to differentiate $\vec{V}_0$ before expanding because Eq. (5.2) is not absolutely convergent; $\int_1\vec{V}_0$ is automatically eliminated. During the numerical integration, the vorticity and the eigenvalues of $\sigma_0^{\alpha\beta}=\nabla^\alpha V_0^\beta+\nabla^\beta V_0^\alpha$ were computed at the origin both from $\vec{V}_0$ directly and after expanding the derivative with Eq. (5.2). The difference was ~10%. We did not explicitly make $\nabla^\alpha V_0^\beta$ transverse in β because $\mathrm{tr}\sigma_0^{\alpha\beta}$ was zero to within 1% at the origin [$\mathrm{tr}\lambda=0$ in Eq. (3.2)]. Equation (5.2) is not so good away from zero. If we had made $\nabla\cdot\vec{V}_0=0$ over the entire box, the shear at the origin would change by 10% which is negligible in comparison with our other errors.

The equations that were integrated numerically result from Eq. (5.1) by expanding the first two nonlinear terms in the manner described.

$$\frac{\partial A_G^{l,\alpha}}{\partial t}+i2^{l-1}(\delta^{\alpha\beta}-G^\alpha G^\beta/G^2)\times\Big(\sum_{H,G'}C_1^{\delta,\gamma}(\vec{G}-\vec{G}',\vec{H})A_H^{l-1,\gamma}G'^\delta A_{G'}^{l,\beta}+\sum_{H,G'}A_{G'}^{l,\gamma}C_2^\gamma(\vec{G}-\vec{G}',\vec{H})A_H^{l-1,\beta}+\sum_{G'}A_{G-G'}^{l,\gamma}G'^\gamma A_{G'}^{l,\beta}\Big)+(\eta_l+2^{2l}/R)A_G^{l,\alpha}=0\,, \tag{5.3a}$$

$$2\eta_l E_l\equiv\epsilon_{l+1}=i2^{l-1}\sum_{\vec{G},\vec{G}',\vec{H}}A_{-G}^{l+1,\alpha}A_{G'}^{l+1,\gamma}C_2^\gamma(\vec{G}-\vec{G}',\vec{H})A_H^{l,\alpha}\,, \tag{5.3b}$$

where

$$C_1^{\alpha,\beta}(\vec{N},\vec{H})=\begin{cases}(\delta^{\alpha,\beta}-N^\alpha N^\beta/N^2)C(\vec{N},\vec{H}), & N\neq0\\ 0, & N=0\,,\end{cases}$$

$$C_2^\alpha(\vec{N},\vec{H})=\tfrac{1}{2}H^\alpha C(\vec{N},\vec{H})\,.$$

The nonlinear terms (containing the pressure in the $-G^\alpha G^\beta/G^2$ factor) are in the same order as Eq. (5.1a). Equation (5.2) defines $C(\vec{N},\vec{H})$. The first two sums over G' in Eq. (5.3a) are unrestricted while the third is limited to $G-G'$ that are among the arguments of A^l; $G^\alpha, H^\alpha=0,\pm1$ and $N^\alpha=0$, $\pm1,\pm2$. All dependence on the physical wave vector or the box size is contained in 2^{l-1}. The equation for η_l is real, except for roundoff errors, because $C^\alpha(-\vec{N},-\vec{H})=-C^\alpha(\vec{N},\vec{H})$. The first and third terms conserve the energy. It will prove useful to have explicitly the equation for E_l, that Eq. (5.3) implies ($R=\infty$):

$$\frac{\partial E_l}{\partial t}=\epsilon_l-2\eta_l E_l\,. \tag{5.4}$$

The rate energy enters shell l from $l-1$ is denoted by ϵ_l. The analytical definitions of η_l and ϵ_l would become somewhat ambiguous had we included next nearest shell couplings or terms such as $\vec{V}_{l-1}\cdot\nabla\vec{V}_{l+1}$.

If it were possible to integrate a realistic number of shells (~20) simultaneously, energy could be added to the system at a constant rate ϵ, or the first shell could evolve undamped ($\eta_1=0$, $E_1=\mathrm{const}$) and supply a random shearing to the second shell. Alternately, instead of setting up a stationary distribution, the first shell could be started with a fixed amount of energy that would decay slowly to zero. The succeeding shells should equilibrate to some locally defined ϵ. For a prescribed Reynolds's number, $2^{2l}/R$ will eventually dominate η_l and terminate the cascade.

Because we were limited to four shells, assumed to be in the inertial range ($R=\infty$), the choice of a source and sink of energy requires care. It appeared rather difficult to extract, from only four shells, a universal distribution if they were not stationary; so the first of the stationary models was used. Feeding energy into the first shell at a constant rate provides more useful information from a limited number of shells than using the

first shell at constant energy to generate a random shear. Equation (5.3) becomes for $l=1$:

$$\frac{\partial A_G^{1,\alpha}}{\partial t} - \epsilon \frac{A_G^{1,\alpha}}{2E_1} + i\left(\delta^{\alpha\beta} - \frac{G^\alpha G^\beta}{G^2}\right) \times \sum_{G'} A_{G-G'}^{1,\gamma} G'^{\gamma} A_{G'}^{1,\beta} + \eta_1 A_G^{1,\alpha} = 0 \quad (5.5a)$$

and

$$\frac{dE_1}{dt} = \epsilon - 2\eta_1 E_1 . \quad (5.5b)$$

The single number ϵ replaces the 78 modes that would normally drive any shell in the inertial range. The function $\eta_4(t)$ determines the energy sink in the fourth shell. Without knowing ϵ_5, we parametrize η_4 in terms of known quantities:

$$\eta_4(t) = 2^{2/3}\{\langle\eta_3\rangle + \gamma[\eta_3(t-\delta) - \langle\eta_3\rangle]\} . \quad (5.6)$$

The scale factor γ, the average of η_3, $\langle\eta_3\rangle$, and the time lag δ are determined self-consistently. The choice of an energy sink is more delicate than picking an energy source. The reasons favoring Eq. (5.6) are given in the following subsection. The actual parameters and the accuracy of the self-consistency are contained in subsection C. This completes the specification of the model equations that were integrated numerically. Note that (5.3), (5.5), and (5.6) are deterministic; there are no stochastic forces. The eddy viscosity is determined to conserve energy during the transfer between shells but the energy source in shell 1 need not balance the sink in shell 4 at every instant.

It is possible to qualitatively estimate how several omitted terms would affect the efficiency of the energy cascade (or equivalently $\langle E_l\rangle$) represented by Eq. (5.3). Their effect on the fluctuations is included in the section on intermittency. When $b=2$, phase-space constraints no longer appreciably diminish either $\vec{V}_{l-1}\cdot\nabla\vec{V}_{l-1}$ or $\vec{V}_l\cdot\nabla\vec{V}_{l+1} + \vec{V}_{l+1}\cdot\nabla\vec{V}_l$ in $d\vec{V}_l/dt$. They may be considered together, since to the extent that $\vec{V}_{l-1}\cdot\nabla\vec{V}_{l-1}$ changes E_l, $\vec{V}_{l-1}\cdot\nabla\vec{V}_l + \vec{V}_l\cdot\nabla\vec{V}_{l-1}$ (omitted from $d\vec{V}^{l-1}/dt$) causes the opposite change on E_{l-1}. If $\vec{V}_{l-1}\cdot\nabla\vec{V}_{l-1}$ is multiplied out and Eq. (5.2) used where necessary to convert into the basis of shell l, simply counting terms with their Fourier coefficients indicates $\vec{V}_{l-1}\cdot\nabla\vec{V}_{l-1}$ is one half of the first two terms in Eq. (5.3a) when $E_{l-1}/E_l = 2^{2/3}$.

Our approach depends on the locality of the cascade and the existence of a characteristic time that decreases with l, i.e., $\eta_{l+1} \gg \eta_l$; even though for $b=2$ the percentage corrections to either approximation are $\sim 2^{-2/3}$. From this viewpoint, the contribution of $\int_l V_l^\alpha \vec{V}_{l-1}\cdot\nabla\vec{V}_{l-1}^\alpha$ to dE_l/dt is small, of variable sign, and leads on average to algebraic rather than exponential growth in time.[16] For reasons of consistency it is awkward to include $\vec{V}_{l-1}\cdot\nabla\vec{V}_{l-1}$ because the companion term, $\vec{V}_{l-1}\cdot\nabla\vec{V}_l + \vec{V}_l\cdot\nabla\vec{V}_{l-1}$, in shell $l-1$ does not act like an eddy damping. This is easiest to see diagrammatically since an eddy damping follows only when both intermediate states belong to higher shells. The mean-field exponents are not affected by $\vec{V}_{l-1}\cdot\nabla\vec{V}_{l-1}$.

The second major omission was to neglect any coupling between next nearest shells. The magnitude of this coupling was estimated by numerically computing the eigenvalues of $\sigma_{l-1}^{\alpha\beta} = \nabla^\alpha V_{l-1}^\beta + \nabla^\beta V_{l-1}^\alpha$, $\sigma_{l-2}^{\alpha\beta} = \nabla^\alpha V_{l-2}^\beta + \nabla^\beta V_{l-2}^\alpha$, and $\sigma_{l-1}^{\alpha\beta} + \sigma_{l-2}^{\alpha\beta}$ at the origin of box l. The model of Sec. III implies that these eigenvalues are a good measure of the rate of energy transfer. The two contributions to the shear applied to box l depend on the energy and spatial distribution of velocity in boxes $l-1$ and $l-2$. (One must also include a contribution to η_l from shell $l+2$.) Typically the shear from $l-2$ is slightly larger than the general estimate $\sigma_{l-2} \sim 2^{-2/3}\sigma_{l-1}$, for $E_{l-2}/E_{l-1} \sim 2^{2/3}$ would imply; probably because the expansion for $e^{i2^{l-3}\vec{G}\cdot\vec{r}}$ in $e^{i2^{l-1}\vec{G}\cdot\vec{r}}$ analogous to Eq. (5.2) is somewhat better convergent. Of course, if $E_{l-1}/E_{l-2} \ll 2^{-2/3}$, the shear of shell $l-2$ will dominate. The eigenvalues of $\sigma_{l-2}^{\alpha\beta} + \sigma_{l-1}^{\alpha\beta}$ for $E_{l-2}/E_{l-1} \sim 2^{2/3}$ are on the average only 30% larger than those of $\sigma_{l-1}^{\alpha\beta}$ rather than the 40%–60% one might have thought by comparing $\sigma_{l-2}^{\alpha\beta}$ with $\sigma_{l-1}^{\alpha\beta}$. This is expected, since when adding two random uncorrelated matrices the variances of the elements add rather than the elements themselves.

B. Stability and intermittency

Although only a subset of Eq. (5.3) is actually integrated, it is useful to have a general understanding of the complete hierarchy. A very qualitative but global analysis of the stability of Eq. (5.3) eliminates a number of parametrizations of η_4 that might appear as satisfactory as Eq. (5.6). The numerical results on four shells are then used to illustrate a qualitative explanation of intermittency.

When Eq. (5.3) is integrated forward in time, "observables" such as E_l and ϵ_l will fluctuate along with the velocity amplitudes. Of course, if one applies mean-field assumptions, Kolomogorov's results are recovered. If the much weaker assumption of stationarity is made, Eq. (5.4) can be averaged by integrating over some long time and normalizing. The average value of ϵ_l is the same in all shells:

$$\epsilon = \langle\epsilon_l\rangle = 2\langle\eta_l E_l\rangle . \quad (5.7)$$

Equation (5.7) does not imply, as it does in mean-field theory, that $\langle \eta_l \rangle$ and $\langle E_l \rangle^{-1}$ scale with the same exponent since they may be anticorrelated.

A qualitative analysis of why Eq. (5.3) is stable in spite of potentially large fluctuations is related to the arguments that led to the equations themselves. It reinforces our contention that the terms retained contain the essential physics. The key result (confirmed numerically) is that the vortex-stretching term always transfers energy to higher wave numbers even in the presence of large fluctuations, e.g., $\epsilon_l(t) > 0$. Numerically, a strictly nearest neighbor cascade is quite inadequate when $E_{l-1}/E_{l-2} \ll 2^{2/3}$, but nevertheless is stable. When only a potential divergence is at issue, the order of magnitude of ϵ_l can be estimated from E_{l-1} and E_l. Equation (5.4) becomes (restoring the Reynolds's number)

$$\frac{\partial E_1}{\partial t} = \epsilon - 2E_2(E_1)^{1/2} - \frac{4}{R}E_1 . \tag{5.8}$$

$$\frac{\partial E_l}{\partial t} = 2^l E_l (E_{l-1})^{1/2} - 2^{l+1} E_{l+1} (E_l)^{1/2} - \frac{2^{2l}}{R} E_l , \quad l > 1 .$$

The signs of the various terms are dictated by energy conservation and the direction of energy transfer. The wave vector appears through the factor 2^l.

We do not wish to imply that (5.8) constitutes a sensible model of the cascade. When the equations are integrated numerically, the energy of some intermediate shell collapses to zero. The total energy in the preceding shells then grows as ϵt, neglecting viscosity, while the total energy in the succeeding shells decays to zero. When (5.3) is integrated, it is very unlikely that all 78 velocity modes would ever by simultaneously zero and a collapse has never been observed. Also when a term $\vec{V}_{l-1} \cdot \nabla \vec{V}_{l-1}$ is included in (5.1a) E_l would grow algebraically in time if it were ever nearly zero.[16] We will use (5.8) only to show that large fluctuations relax back towards equilibrium. Only in this respect is (5.8) an adequate representation of (5.3). In the following section we discuss why (5.3) is a reasonable model of intermittency even though its mean-field version, (5.8), collapses.[17]

To return to the possibility of a runaway in (5.8) when all energies are positive, assume $E_{m+1} \lesssim E_m \ll E_{m-1}$ and E_{m-2} is slowly varying:

$$\frac{\partial E_{m-1}}{\partial t} = 2^{m-1} E_{m-1} (E_{m-2})^{1/2} - 2^m E_m (E_{m-1})^{1/2}$$

$$\frac{\partial E_m}{\partial t} \simeq 2^m (E_{m-1})^{1/2} E_m .$$

Initially E_{m-1} will be undamped and increasing, the precise manner depending on the preceding energies. However, E_{m-1} varies, E_m increases as $\exp(\int^t 2^m (E_{m-1})^{1/2})$ until by the same argument $E_{m+1} \sim (E_m E_{m-1})^{1/2}$, and the damping of E_m by E_{m+1} becomes important. In other words, E_m tends to catch up with E_{m-1}.

A more complex example occurs if $E_{m+1} \sim E_{m-1}$ and $E_m \ll E_{m-1}$. Initially, E_m will decrease algebraically because the damping $\sim (E_m)^{1/2}$ while the driving $\sim E_m$. [This suggests that in certain cases Eq. (5.8) or (5.3) will amplify fluctuations.] Simultaneously, however, E_{m-1} will increase and E_{m+1} decrease (provided all other energies are near their average values). It is possible that E_m will reach zero and remain there until E_{m+1} has declined to zero. In the presence of a small amount of noise, we again have the configuration $E_{m+1} \lesssim E_m \ll E_{m-1}$. The point $E_m = 0$ is a singular point of Eq. (5.8). If E_m were to become slightly negative, it would go to $-\infty$. Only the positive solution is physical.

To do a numerical calculation with only four shells, whatever ansatz is used to find η_4 must not only fit the computed data when applied to η_3 or η_2 but incorporate the stabilizing features of the complete hierarchy of equations. The first requirement does not insure the second. Equation (5.3b) suggests an alternative to Eq. (5.6); estimate ϵ_5 from ϵ_4 and use $\eta_4 = \epsilon_5/2E_4$. Although the equation,

$$\epsilon_{l+1}(t) = (1+\gamma)\epsilon_l(t-\delta) - \gamma\epsilon_l(t-\delta') , \tag{5.9}$$

fit the computed data for $l = 2$ and 3 at least as well as Eq. (5.6), the cascade collapsed. The parameters δ and δ' are the two discrete time intervals that best match the lag of ϵ_{l+1} behind ϵ_l (see Fig. 1). Clearly, Eq. (5.9) implies the correct mean for ϵ_{l+1}, and γ is used to adjust

$$\langle \epsilon_{l+1}^2 \rangle / \langle \epsilon_l^2 \rangle .$$

(Angular brackets denote connected correlation functions.)

When Eq. (5.9) was applied, E_4 became and remained much larger than E_3. In reality, ϵ_5 should become much larger than Eq. (5.9) implies, rather than being of order ϵ_4 which is depressed by E_3; and E_4 would then decrease as $\int^t (\epsilon_4 - \epsilon_5)$. As long as E_3 remained small, E_2 grew as the expense of E_1 because $\epsilon_3 \ll \epsilon_2$. The integration was continued until E_2 was unreasonably large although E_3 remained less than E_4.

Equation (5.6) is not susceptibile to this instability. If $E_3 \ll E_4$ and $\epsilon_4 \sim \epsilon_5$, as permitted by Eq. (5.9), $\eta_3 \gg \eta_4$. Switching to Eq. (5.6) would make $\eta_4 \sim \eta_3$, $\epsilon_5 \gg \epsilon_4$, and E_4 would decrease. In the opposite limit $E_4 \ll E_3$, $\epsilon_4 \gg \epsilon_5$, and the cascade would again reequilibrate.

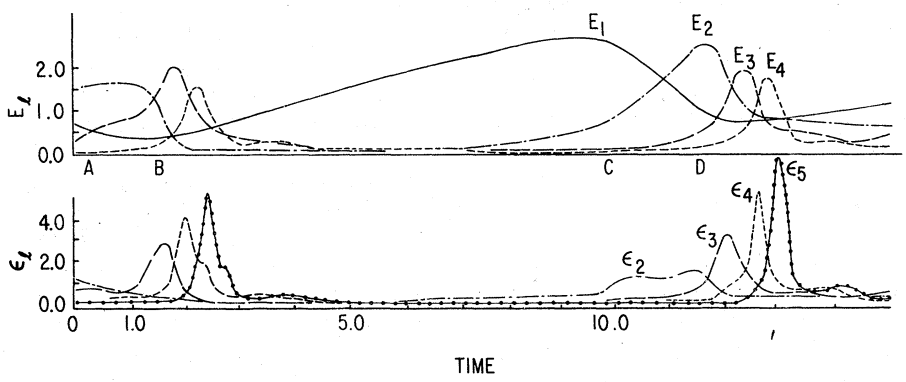

FIG. 1. Numerical data for $\gamma=1.2$ Eq. (5.6) showing E_l and ϵ_l, [$\epsilon_5 \equiv 2\eta_4 E_4$, see Eq. (5.6)], at corresponding times. The averages of E_l and $\epsilon = \langle \epsilon_l \rangle$ are 1.23, 0.74, 0.40, 0.22, and 0.38 respectively; $\langle E_1 \rangle$ and ϵ determine the unit of time. The origin of time was shifted to zero. All dependence on the initial conditions has disappeared.

The origin of intermittency in turbulent flows has been the subject of considerable debate since the original papers of Kolmogorov and Oboukhov.[4] The viewpoint generally adopted, though with many variations, assumes a stepwise cascade and intermittency corrections that build up multiplicatively.[7] One works directly with a probability distribution that contains all of the equal time correlation functions and most of the physically interesting information. Unfortunately, without making some nontrivial use of the Navier-Stokes equations, there are a multitude of equally viable models.[5]

Working with equations of motion has led to a dynamical explanation of intermittency that makes essential use of the Navier-Stokes equations. The simplicity of a probability distribution has been lost and can only be recovered by preparing a histogram from our time series. It is more reliable to compute correlation functions directly as time averages, but there is no obvious relation among all their exponents.

Operationally, intermittency is the amplification of fluctuations in successive shells as the energy cascades to shorter distances. The buildup of intermittency in Eq. (5.3) (and we believe also in the Navier-Stokes equations) for states "near" Kolmogorov's follows from several simple properties listed below. When the fluctuations become large, however, we have to rely on the numerical integration and general stability arguments.

(i) Intrinsic intrashell fluctuations induce variations into the stress tensor that drives the succeeding shell.

(ii) The energy decreases exponentially with shell number (i.e., algebraically in wave number) and the characteristic frequency increases exponentially.

(iii) The cascade is local, and the direction of energy transfer is to shorter distances.

According to (i), ϵ_l and therefore E_l vary in time. Because ϵ_l depends primarily on the shear, σ_{l-1}, in the preceding shell rather than its energy, there will be additional variability to the extent σ_{l-1} is not a function of E_{l-1}. Models with very few degrees of freedom per shell tend to either have no intrinsic fluctuations or collapse. If fluctuations did not amplify down the cascade, the mean-field exponents would probably still apply.

The development of intermittency can be most easily understood in reference to Fig. 1. At point C (D), E_2 (E_3) attains its mean and continues to grow at a rate determined by ϵ_2 (ϵ_3) because ϵ_3 (ϵ_4) is small. Not only does shell $l+1$ respond faster than shell l (successive peaks are sharper and more closely spaced), but a given amount of energy causes a bigger percentage fluctuation in E_{l+1} than E_l. Energy passes through shell $l+1$ faster than shell l so that successive energy maxima may decrease but not by $2^{2/3}$. Locality is important because any excess energy in l has to pass through $l+1$ before being dissipated. The time lag between energy maxima in successive shells causes each to overshoot its mean. As long as E_{l+1} is sufficiently small, E_l will grow at the expense of E_{l-1}.

The shell energies after the pulse of energy in shell 1 has passed down the cascade depend sensitively on the relative energies at point C. If E_3 were initially larger, it would have caught up sooner with E_2, which would not have grown as much as it did at the expense of E_1. The fact that E_1 grows secularly immediately after E_2 is reduced to half its maximum is an artifact of the first shell into which energy is fed at a constant rate, Eq. (5.5). More typical is E_2 which continues to decrease even after E_3 and E_4 have peaked because E_1 was reduced to below its mean.

It is instructive to compare the first series of peaks with those beginning at C. Both E_1 and E_2 have rather gentle maxima, but when E_3 reached its mean at point A, E_4 was nine times smaller than it was when E_3 was again at its mean at point D. (A log plot would make this easier to see.) It then took twice as long (after point A) for E_4 to reach its mean (point B) than it did after

point D, and consequently E_3, relative to E_1 and E_2, has a larger and sharper peak in the former case. From point B, until it began to increase again, E_2 was smaller than E_3 and E_4. Shells 3 and 4 respond rather slowly until point C because $\eta_l \sim 2^l (E_l)^{1/2}$ or $2^{l-1}(E_{l-1})^{1/2}$. The energy in the second shell will continue to decline along with ϵ_2 until $E_3 < E_2$. Simultaneously, the first shell will grow monotonically but only as ϵt rather than exponentially. The length of time E_2 remains small determines how large a reservoir of energy builds up in shell 1. Large peaks in ϵ_l are always preceeded by a period during which some $E_{m<l}$ is very small. Note that E_2 remains larger than E_3 and E_4 after the second set of peaks, and there are no further prominent features for an interval $2\frac{1}{2}$ times the length of Fig. 1. The cascade amplifies the normalized energy fluctuations; only correlation functions of $E_l/\langle E_l\rangle$ are guaranteed to have a positive exponent.

The maxima of ϵ_m typically fall between those of E_{m-1} and E_m, e.g., when E_{m-1} is falling and E_m increasing. There is an alternative version of our intermittency argument for ϵ_l that is more reminiscent of mean-field theory. If ϵ_m fluctuates, succeeding shells respond more rapidly and equilibrate to a local value of ϵ. Fluctuations of $\epsilon_{l>m}$ ride on those of ϵ_m.

The curve labeled ϵ_5 in Fig. 1 is actually just twice E_4 times η_4 in Eq. (5.6). There is no parameter in (5.6) to control the width of peaks in ϵ_5 which are wider than scaling would predict. The phase lag δ as well as $\gamma > 0$ make the variance of ϵ_5 larger than $\langle \epsilon_4^2 \rangle$. If a large η_3 signals a large energy loss to shell 4 (e.g., $E_3 \sim \langle E_3 \rangle$, $\epsilon_4 \gg \epsilon$), η_4 will not respond for a time δ, modeling the growth time of E_5 and ϵ_5, and allowing E_4 to grow more than it would if $\delta = 0$. Similarly, if a large η_3 occurs because E_3 is small and $\epsilon_4 \sim \epsilon$, energy will continue to flow from 3 to 4 for a time δ further depressing E_3. When η_4 begins to increase, η_3 will have already gotten somewhat larger (E_3 smaller and E_4 larger) than would otherwise have happened. After a delay of δ, ϵ_5 will have a peak. The phase lag has a similar effect when η_3 is small.

To predict from a few initial correlation functions if a given energy will grow or decay is only possible in extreme cases and over short periods of time. It seems reasonable intuitively and from the numerical data that the larger fluctuations require a more special confluence of parameters at some instant in the cascade. The larger the fluctuation, the longer the time interval between them. There appears to be no limit on how large a fluctuation might occur in a sufficiently long interval. This circumstance need not affect the low-order moments, but higher-order correlation functions will depend increasingly on these rare fluctuations.

By understanding why the cascade fluctuates, it is possible to qualitatively predict the effects of several neglected terms. When $E_l \ll E_{l-1}$, $|\vec{V}_{l-1} \cdot \nabla \vec{V}_{l-1}| \gg |\vec{V}_l \cdot \nabla \vec{V}_{l-1} + \vec{V}_{l-1} \cdot \nabla \vec{V}_l|$ so including the former term will lessen the periods during which E_l is unusually small, i.e., $\lesssim 10^{-2} E_{l-1}$. Although variances and higher connected cumulants are expected to decrease, small fluctuations about the mean-field energies should still be amplified.[16]

Next nearest neighbor energy transfer can act in two ways on ϵ_l. If $E_l \ll E_{l-1}$, E_{l-1} will not grow as rapidly as in our model when there is some direct energy transfer to E_{l+1}. Similarly, ϵ_{l+1} receives contributions from shells l and $l-1$ that tend to average out the fluctuations in either shell. On the other hand, direct transfer between $l-1$ and $l+1$ might accentuate the percentage fluctuations in $l+1$, since by an earlier argument, shell $l+1$ is both faster and contains less energy relative to $l-1$ than shell l. If $E_l \ll E_{l+1} \lesssim E_{l-1}$, direct transfer between E_{l-1} and E_{l+1} would maintain the latter which would then continue to depress E_l.

C. Numerical results for four shells

In principle, it would not be necessary to integrate a realistic number of shells (~20) simultaneously to study the inertial range, if a self-consistent calculation could be done on several shells. This would require an energy source that coupled realistically to shell 1 and responded to fluctuations in E_1 in addition to being random itself. Instead, energy was fed into the first shell at a constant rate [Eq. (5.5)], and consequently the fluctuations of E_1 differ from $E_2 - E_4$, Fig. 1. The fluctuations of the other shells are qualitatively similar in shape but become increasingly singular. To anticipate, Table I shows that correlation functions can be scaled from shell to shell with the same exponents and, we presume, continue to scale if more shells were added. The internal consistency of our data is the best evidence that it actually relates to the inertial range.

There are two free constants in any numerical calculation that determine the length and time scales. The former was fixed to make the minimum wave number in the first shell one and the latter by setting $\epsilon = 0.38$ in Eq. (5.5). The average energy within mean-field theory is now a universal constant. The Kolmogorov constant C_K is conventionally defined by an equation for the energy spectrum,

TABLE I. Exponents from four-shell model. The parameter γ in (5.6) was varied to achieve self-consistency. The three determinations of each exponent come from the ratio of correlation functions, averaged over $\Delta t \sim 150$, in successive shells. The range of values in parentheses are the minimum and maximum exponents found for 10 subintervals with $\Delta t \sim 75$. The tabulated exponents all vanish in mean-field theory.

Definition of exponents	Quantity tabulated	$\gamma = 1.1$	$\gamma = 1.2$	$\gamma = 1.3$
$\langle E_l \rangle \sim 2^{-(2/3+\zeta)l}$	ζ	0.0 (−0.5, 0.1)	0.1 (0.0, 0.5)	−0.1 (−0.2, 0.0)
		0.2 (0.2, 0.3)	0.2 (0.0, 0.3)	0.2 (0.1, 0.3)
		0.2 (0.1, 0.2)	0.2 (0.2, 0.2)	0.3 (0.2, 0.4)
$\langle \eta_l \rangle \sim 2^{(2/3-\delta)l}$	δ	0.4 (0.4, 0.7)	0.1 (−0.1, 0.2)	0.1 (−0.1, 0.5)
		0.3 (0.0, 0.4)	0.1 (0.0, 0.3)	0.2 (0.0, 0.4)
		0.0 (0.0, 0.0)	0.1 (0.0, 0.1)	0.1 (0.1, 0.2)
$\langle E_l^2 \rangle \sim 2^{-\phi l}$	$\frac{4}{3} + 2\zeta - \phi$	0.8 (−0.3, 1.0)	1.1 (0.7, 1.6)	0.9 (0.6, 1.0)
		−0.1 (−0.4, 0.4)	0.3 (−0.1, 0.6)	1.1 (0.6, 1.3)
		0.9 (0.6, 1.2)	0.8 (0.7, 0.9)	0.5 (0.1, 0.9)
$\langle \epsilon_l^2 \rangle \sim 2^{\mu l}$	μ	0.4 (0.1, 1.2)	0.9 (0.8, 1.2)	1.0 (0.4, 1.2)
		1.0 (0.6, 1.2)	0.8 (0.6, 0.9)	1.1 (0.9, 1.2)
		0.4 (0.4, 2.0)	0.6 (0.6, 0.6)	0.7 (0.6, 0.7)
$\langle \epsilon_l^3 \rangle \sim 2^{\mu_3 l}$	μ_3	0.2 (0.0, 2.6)	2.2 (1.7, 2.8)	2.1 (0.2, 2.2)
		2.5 (1.3, 2.6)	1.7 (1.4, 1.7)	2.6 (2.0, 3.1)
		0.7 (0.7, 1.2)	1.1 (1.0, 1.1)	1.3 (1.2, 1.3)

$$E(k) = C_K \epsilon^{2/3} k^{-5/3}. \tag{5.10}$$

Had our calculation been done by using the first shell, undamped and at constant energy, to produce a random shear on the second shell, E_1 would fix the time scale and ϵ becomes the derived universal quantity. Equation (5.10) requires modification if mean-field theory does not hold for $E(k)$, but the deviations are small and, $C_K \sim 2$, is determined by fitting Eq. (5.10) to the experimental data.[18] If a fit is made to

$$E_l = \int_{2^{l-1}}^{2^l} E(k)\,dk$$

for $l = 2, 3$, then $C_K \sim 3.5$. The Kolmogorov constant measures the efficiency of the cascade. A more efficient cascade will have lower energies if ϵ is the same, or if the same energies prevail, dissipate more energy/time. The terms we have neglected, intuitively, should decrease C_K.[16]

The numerical integration was begun by generating a random set of initial-velocity amplitudes scaled to agree with mean-field theory. The integration routine was an IBM coded version of Hamming's fourth-order predictor-corrector method. The program had the capability of subdividing the initial step size h until the estimated truncation error was less than a predetermined bound. An initial step size of $h = 0.12$ was optimal, in that when energies were near their mean-field values, the program used the full step, but during large fluctuations made as many as three successive bisections of the original increment ($h' = 0.015$). To integrate four shells forward 100 time units required 1150 steps on the average and 35 min of C.P.U. time on an IBM 370/168 or 200 min on an IBM 360/65. Approximately 60% of total C.P.U. time was spent computing the expansion of V_{l-1} with Eq. (5.2) and an additional 25% assembling the right-hand side of Eq. (5.3a). There is no reason to make the accumulated truncation error less than 10 ~ 20% of the average energies over the time (~2–3) for a pulse of energy to pass from shell 1 to shell 4 (see Fig. 1). Noise of this magnitude might represent the presence of other boxes in the same shell, and if it had any effect on exponents would be grounds for questioning the model. More can be learned from a given amount of computer time by making a moderate truncation error but accumulating as much data as possible to improve the statistics. Each run in Table I represents ~170 time units. Times less than ~15 were excluded from the averages.

Table I gives data for three different values of γ in Eq. (5.6). The uncertainties quoted reflect only the statistical error. This was computed by breaking up the complete time record into ten approximately independent segments each half as long. Within each segment, averages and variances were determined separately and from their ratios the exponents. The principal entries in the table are the exponents determined from the entire interval and in no sense represent an average of those of the subintervals. The data for $\gamma = 1.1$ are poorer than the rest because of an unusually large fluctuation. Equation (5.6) requires a self-consistent value of $\langle \eta_3 \rangle$. In prac-

tice we used $\langle\eta_3\rangle = 0.45$ in all three runs. The computed averages (and uncertainties) were 0.41 (0.38–0.42), 0.43 (0.39–0.47), and 0.43 (0.42–0.46) for $\gamma = 1.1$, 1.2, and 1.3, respectively. The fluctuations in η_3 averaged over $\Delta t \sim 15$–20, several correlation times of E_2 or E_3, would be twice those reported. The difference between 0.41 and 0.45 for $\gamma = 1.1$ is immaterial.

The variance of ϵ_l clearly increases with γ, although $\langle\epsilon_5^2\rangle$ does not increase relative to $\langle\epsilon_4^2\rangle$ as was hoped. [$\epsilon_5 \equiv 2n_4E_4$, see Eq. (5.6).] The second and third determinations of μ in Table I are within the uncertainties of an individual run, but the trend for the three runs is probably real. Higher moments of ϵ_5 are also low. Note that $\langle\eta_4\rangle \neq 2^{2/3}\langle\eta_3\rangle$ as expected from Eq. (5.6). This resulted from a bias in selecting the most appropriate value of $\eta_3(t-\delta)$ from a discrete set of times. It was not corrected since the biased value was in better agreement with the other data. The variance of E_2 appears high relative to E_1. This is probably a shortcoming of the approximation $\epsilon_1 \equiv \epsilon$, Eq. (5.5). The "best" value of γ is 1.2 for which the three sets of exponents for $\langle E_l\rangle$, $\langle\eta\rangle$, and $\langle\epsilon^2\rangle$ are in good agreement, implying self-consistency.

The most striking qualitative features of Table I is that μ deviates far more from its mean-field value, 0, than do the exponents for $\langle\eta_l\rangle$ and $\langle E_l\rangle$. The exponent of $\langle E_l\rangle$ is greater than 0.67 and increases from $\gamma = 1.1$ to 1.3 with either μ or $\langle\epsilon_l^2\rangle$ itself. About all that can be concluded from our data is $\zeta > 0$, and even this statement may be an artifact of our model.[16] The vorticity exponents agree with those for the energy to about 5%. The exponent for $\langle\eta_l\rangle$ appears less than 0.67, but the same caveats apply. Table II contains our best estimate of the various exponents and the predictions of the log-normality model for comparison.

The exponent commonly called μ that relates to the fluctuations in the averaged dissipation is approximately 0.5 experimentally. One in principle measures the fluctuations of the dissipation rate ϵ_r averaged over a small volume v_r and extracts μ from a graph of $\langle \int \epsilon_r \int \epsilon_r \rangle$ vs v_r. Alternatively one can plot the correlation function of the dissipation rate at two nearby points as a function of their separation.[7] The average dissipation rate is not an inertial range quantity while the energy transfer, ϵ_l, from shell to shell is.[5] In our notation, ϵ_r is the arithmetic average of 2^{3n} realizations of ϵ_{l+n} all contained in the box l that best approximates v_r, with $n + l \sim \ln_2 \Lambda_K$. The fluctuations of the ϵ_{l+n} are uncorrelated for times $\ll \eta_l^{-1}$ but averaged over times $\sim \eta_l^{-1}$ reflect the fluctuations of ϵ_l. Unfortunately as R and $n \to \infty$, l fixed, the central limit theorem does not generally imply that

$$2^{-3n} \sum_{n \in \text{box } l} \epsilon_{l+n} \sim \epsilon_l \ ,$$

and the exponents of ϵ_l and ϵ_r may not be the same as we have assumed.

The predictions of the log-normal theory about the relation of ϵ_l to ϵ_r are ambiguous.[7] Frisch, Sulem, and Nelkin have also proposed that μ be identified with the fluctuations in the energy transfer rate.[8]

The connected third-order moment $\langle\epsilon_l^3\rangle$ (Table I) is a measure of deviations from a Gaussian distribution. It suggests that the distribution of ϵ_l becomes more skewed toward positive values as l increases. Furthermore, $\mu_3 > \frac{3}{2}\mu$ implies that the fluctuations of higher correlation functions become singular more rapidly at short distances.

Figures 2(a)–2(c) plot distributions of ϵ_l, $\ln\epsilon_l$, and $\ln E_l$ for $\gamma = 1.2$ redrawn from histograms of our time series data. The trend in ϵ_l inferred from μ_3 is apparent. Increasing fluctuations lead to a build-up of probability near the origin, because $\epsilon_l > 0$, and a longer tail, $\langle\epsilon_l\rangle = \epsilon$. The first inequality, $\epsilon_l > 0$, is slightly violated for 2.5% or our data when $E_{l-1}/E_l \lesssim 10^{-2}$, and a reverse cascade is not unreasonable. After only a few cascade steps, the distribution of $\ln\epsilon_l$ is more nearly symmetric but contains a tail to $-\infty$. The log-normal assumption would give a reasonable representation for high moments of ϵ_l for which the weight near zero is unimportant. The data for E_l shows the same trends but they are not as pronounced. Note also that the distributions of $\ln\epsilon_3$ and $\ln E_3$ are similar in accordance with Kolmogorov's assumption, $E_r \sim (\epsilon_r r)^{2/3}$.[4]

TABLE II. Comparison with log-normality predictions.

Exponent	ζ	δ	$\frac{4}{3} + 2\zeta - \phi$	μ	μ_3
"Best" value of Table I	0.1 ± 0.1	0.1 ± 0.1	0.7 ± 0.3	0.8 ± 0.2	1.7 ± 0.5
Log-normality prediction (Ref. 4)	$\mu/9$	$\mu/9$	$4\mu/9$	μ	3μ

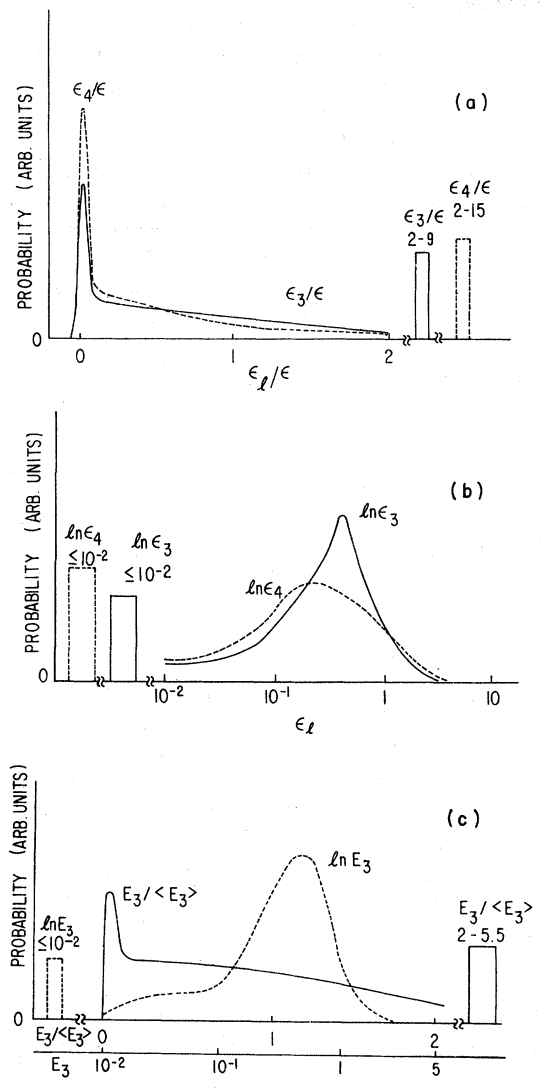

FIG. 2(a–c). Probability distributions prepared from histograms of data for $\gamma = 1.2$. The total probability from all data that fell beyond the range of the abscissa is represented by a single rectangle drawn to scale with the minimum and maximum of the data it represents indicated. The area under the two curves and their respective rectangles in each figure are the same. Only the algebraic scales are in units of the average of the quantity plotted.

VI. CONCLUSION

An analysis of the Navier-Stokes equations, supported by numerical calculations, has revealed a number of generally accepted semiquantitative properties of isotropic turbulence that lacked theoretical support. Our equations are inherently three dimensional and simplified to the point of containing only the vortex-stretching terms and an eddy viscosity. These terms alone have led to a local cascade that is stable in spite of large fluctuations. Vortex-stretching physics is essential to the energy transfer process and renormalized versions of Taylor's model were not found useful. Mean-field theory is invalid not simply because there are fluctuations, but because for a local cascade (and for small fluctuations the cascade is local) they amplify. If the fluctuations become large, energy transfer between next-nearest shells exceeds the nearest-neighbor transfer part of the time. The nearest-neighbor model clearly overestimates the fluctuations, but even when energies differ by a factor of 100 from their mean, $\epsilon_l > 0$. The irreversibility of the cascade is due to the comparatively rapid equilibration of small scales while they are simultaneously sheared by the larger eddies (Sec. III). Because ϵ_l is almost always positive, its mean is independent of l and its fluctuations increase with l; a log-normal distribution is not a bad approximation.

Viewed in time, or in space at a fixed time, the spectrum of ϵ_l (and presumably the dissipation) consists of a series of bursts. Note that the exponent μ measures how fluctuations are amplified as they cascade to shorter distances. The quiescent periods are necessary to satisfy the constraint $\langle \epsilon_l \rangle = \epsilon$ but have comparatively little effect on the second and higher moments of the ϵ_l distribution. By examining the record in time, one sees qualitatively that a fluctuation can reduce a shell energy to near zero and how then a reservoir of energy builds up in the preceding shell until the first shell recovers and releases it explosively. The corrections to the mean-field exponents come in two sizes: ζ and $\delta \sim 0.1$ and μ between 0.5 and 1.0. This distinction is well established experimentally but the only previous theoretical work we know of has only tenuous connections to the Navier-Stokes equations.[4,6,8]

There is a geometric description of intermittency, primarily developed by Mandelbrot, that has intuitive appeal but makes no quantitative use of the Navier-Stokes equations.[8] As reinterpreted by Frisch and co-workers, one imagines the fluctuations in a passive scalar or the local dissipation rate itself becoming less space filling as their scale decreases. In other words, interaction with a turbulent velocity field not only degrades the scalar fluctuations but at each cascade step causes some spatial segregation into quiescent and active regions.

We are unable to say directly how the fluid would look at any instant of time because we have retained only one box per shell but the above picture is not at variance with our expectations. Assume that in shell $l+1$ we retained the eight boxes con-

tained in the preceding l box. When the energy in l begins to grow all eight realizations of box $l+1$ will respond but not necessarily in phase. Their response is more rapid than shell l and depends on the local shear and initial conditions which will vary. The geometric picture predicts a fraction $1-2^{-\mu}$ of the $l+1$ boxes will be quiescent at any instant given that the l box they occupy is excited.

A calculation that retained eight realizations of box $(l+1)$ would be able to treat the intrashell couplings quite accurately and could very well lead to greater intermittency than we have found. Because the eddy damping is determined by the energy entering all eight boxes, rather than eight times the energy entering one $l+1$ box as assumed until now, a few of the $l+1$ boxes could grow enormously before appreciably damping the l box driving them. Phase locking among equivalent boxes, i.e., strong intrashell coupling, would reduce the intermittency. Our numerical calculations effectively treat the reaction of shell $l+1$ back on shell l as if the intrashell coupling were strong, but neglect it while following the evolution of the one box retained in shell $l+1$. In a mean-field approximation one could model this effect by coupling an energy reservoir to each box. This should decrease the intermittency from what we have found. Thus treating intrashell effects exactly has two principal effects on the intermittency that are not contained in our approximation; but they tend to cancel.

Our decomposition of the Navier-Stokes equations rests on an unusual choice of coordinates. At each step of the cascade, we go to a new coordinate frame that eliminates the part of the larger scales that is uniform over the box in question. Only the residual shear affects the small scales. These coordinates are trivial to construct numerically. Seventy-eight modes per shell are adequate to describe a local group of eddies of the same characteristic size, although more economical descriptions of the vortex-stretching process appear possible. If the basis functions are known explicitly, there are no free parameters in the equations for the amplitudes.

It has become possible in the last few years to directly solve the Navier-Stokes equations for the larger scales with up to 10^6 modes in a realistic geometry.[19,20] The coupling to the small scales remains a problem. Equations similar to ours should permit one to simulate the smaller scales and close the equations even when the large scales are anisotropic.

There is a vast literature on analytic theories of turbulence that can only be alluded to. A mode coupling theory in Eulerian coordinates that does not take account of Galilean invariance will not reproduce mean-field theory.[14] When appropriate modifications are made, a "$\frac{5}{3}$ law" is found, but we do not regard this as any more compelling or rigorous than power counting graphs which is equivalent to Kolmogorov's original arguments.[21] Kraichnan has developed a number of approximations that appear more complicated than simple mode coupling.[14] None to our knowledge have exhibited intermittency.

A number of important physical questions are not easily answered by a self-consistent calculation based on only four shells. It is known experimentally that $E(k)$ decreases more rapidly than $k^{-5/3}$ when $k \gtrsim \Lambda_K$. There probably exists a universal scaling function, $\epsilon^{2/3}k^{-5/3}f(k/\Lambda_K)$ in mean-field theory, that would be interesting to calculate. In addition, there should be an exponent analogous to ν that corrects the mean-field relation $\Lambda_K \sim R^{3/4}$.

It must not be inferred from our results that $\epsilon > 0$ when $R \to \infty$.[9,15] Each time a shell is added to the cascade with ϵ fixed as in Eq. (5.5a), E_1 might increase by a factor 2^γ, $\gamma \sim O(\zeta)$. Then to keep E_1 fixed, ϵ should be decreased by $2^{-3\gamma/2}$, implying $\epsilon \sim R^{-9\gamma/8+O(\zeta^2)}$. The decay rate of the largest eddies, ϵ, is not a free parameter, although with only four shells, Eq. (5.5a) is equivalent to the more realistic model in which E_1 is prescribed and generates a random shear that drives the succeeding shells. Because γ is small, a change in E_1 when going from four to five shells at constant ϵ might be an artifact that would disappear if we were able to handle many more shells. The same objection could be raised against our other results, but μ is sufficiently large and to a degree self-consistent that its vanishing appears unlikely.

A tractable method is needed for iterating a description of several cascade steps to map out the entire cascade. If this were possible, one could formulate some notion of "relevancy." It was argued qualitatively, and to some extent checked numerically, that $\vec{V}_{l-1}\cdot\nabla\vec{V}_{l-1}$ and $\vec{V}_{l-2}\cdot\nabla\vec{V}_l + \vec{V}_l\cdot\nabla\vec{V}_{l-2}$ are smaller by a factor $2^{-2/3}$ than the other terms in $d\vec{V}_l/dt$ and are not required for stability. Is there some limit in which they are negligible? Another open question is the existence of scaling laws. There are an infinite number of singular correlation functions, for instance $\langle\epsilon_l^n\rangle$ or $\langle E_l^n\rangle$, $n=2,3,\ldots$, that might all have different exponents. The log-normality models relate all inertial range exponents to μ by postulating a probability distribution for ϵ_l.[4,6]

The most compact description of a turbulent fluid is in terms of a probability distribution that for reasons of economy should be calculated directly rather than prepared from a histogram of a time series. If a probability distribution is calculated recursively, the modes that are integrated out

should be faster than those retained, so as not to introduce progressively more retarded interactions between the remaining modes. Hopefully, the probability at $t+\delta t$ will depend only on the probability at t. Eight realizations of shell $l+1$ would be needed if its damping effect on shell l were not parametrized by an eddy viscosity. A probability distribution, however, describes all eight $l+1$ boxes in each l box and permits one to work from small to large scales.

For many reasons it is necessary to consider the entire cascade rather than only four shells. Even if there was sufficient machine time and storage capacity to integrate a realistic number of shells, one would still have to contend with the decreasing characteristic time in the smaller boxes. For 20 shells, $\eta_{20}/\eta_1 \sim 10^4$ and the variance of ϵ_{20} would be 10^3 times what we found in Fig. 1. There is no reason to choose the time step the same in all shells. Schematically, one would subdivide the hierarchy into subgroups in which the characteristic time varied by a reasonable factor and adjust the time step accordingly. The last group would be integrated several times with a smaller step each time the preceding group was integrated once. As one integrated forward in time, the smallest scales would equilibrate first followed by the larger scales. After sufficiently many shells had equilibrated, the velocity distribution should scale from shell to shell, marking the inertial range.

The intent of this paper is to provide insight into the physical origins of the fluctuation effects that invalidate Kolmogorov's theory. Numerical accuracy was sacrificed in order to reduce the model equations to the simplest possible form without introducing arbitrary adjustable parameters. By partitioning the degrees of freedom into wave-number bands it became easier to visualize the dynamics of the cascade process. Our numerical calculations, however, encompassed only a range of 2^4 in wave number while direct simulations are now capable of handling $\sim (4\pi/3)\times(32)^3$ modes.

In conclusion it is worth while to reiterate the purely computational efficiencies of cascade calculations because many more than four shells can be handled with present day computers. The most obvious is that a simulation requires $N \sim (4\pi/3)2^{3n}$ modes versus $78n$ to encompass n octaves of wave number. With an intelligently written code, the simulation requires $\sim N \ln N$ operations per time step.[22] Our program performs $\sim n \times (78)^2$ operations per step which could presumably be lowered to ~78 ln78 operations if convolutions were computed more efficiently. The maximum time step is limited by the frequency of the smallest scales which depends essentially only on the maximum wave number. The number of time steps controls the statistics. Here the simulation possess a clear advantage since it retains many realizations of the smaller scales compared to the single box retained in the cascade approach. However, the characteristic time of the small scales is least, so integration for a fixed length of time largely compensates for their noisier behavior. The statistical uncertainty is nearly the same for all shells beyond the first in the cascade calculations.

Simulations typically terminate the cascade by including a sufficiently large viscosity to make the Kolmogorov cutoff coincide with the last shell. This is of course the most correct procedure but it means that the last several shells no longer model the inertial range. A cascade calculation should also be terminated in this way but is also quite easy to self-consistently determine the last eddy viscosity. One gains more information on the inertial range at the expense of some arbitrariness. At the present state of our theory, a simulation would provide the most direct check on the many approximations we have had to make. A simulation could also be done on a truncated form of the Navier-Stokes equations that neglects interactions among triples of wave numbers when any two of them differ by more than a factor $b \sim 2$ in magnitude. The results should be directly comparable to a nearest-neighbor cascade calculation and would check the importance of intrashell effects and distortions caused by the eddy damping approximation.

ACKNOWLEDGMENTS

The author has benefited from the comments of U. Frisch, M. Nelkin, D. Nelson, and K. Wilson.

*Permanent address.

[1]P. Martin (private communication).
[2]L. D. Landau and E. M. Lifshitz, *Fluid Dynamics* (Addison-Wesley, Reading, Mass., 1959); A. S. Monin and A. M. Yaglom, *Statistical Fluid Mechanics Vol. I* (M.I.T., Cambridge, Mass., 1973).
[3]K. G. Wilson and J. Kogut, Phys. Rep. C 12, 77 (1974).
[4]A. N. Kolmogorov, J. Fluid Mech. 13, 82 (1962); A. M. Oboukhov, J. Fluid Mech. 13, 77 (1962).
[5]R. H. Kraichnan, J. Fluid Mech. 62, 305 (1974).
[6]A. S. Gurvich and A. M. Yaglom, Phys. Fluids 10, S59 (1967).
[7]M. Rosenblatt and C. Van Atta, *Statistical Models and Turbulence* (Springer-Verlag, New York, 1971); A. S. Monin and A. M. Yaglom, *Statistical Fluid Mechanics Vol. II* (M.I.T., Cambridge, Mass., 1975).

[8]B. Mandelbrot, *Les Objects Fractals: Forme, Hasard et Dimension* (Flammarion, Paris, 1975); B. Mandelbrot in *Proc. Journées Mathématique sur la Turbulence*, edited by R. Teman (Springer-Verlag, New York, 1976); U. Frisch, P. L. Sulem, and M. Nelkin (unpublished).

[9]R. H. Kraichnan, Phys. Fluids 10, 1417 (1967).

[10]P. G. Saffman, in *Topics in Nonlinear Physics*, edited by N. Zabusky (Springer-Verlag, New York, 1968), p. 485.

[11]The physics of vortex stretching is well understood, see for instance, G. K. Batchelor, *An Introduction to Fluid Dynamics* (Cambridge U.P., New York, 1967); and R. H. Kraichnan, J. Fluid Mech. 64, 737 (1974).

[12]The implications of vortex stretching for energy transfer are also discussed in A. A. Townsend, *The Structure of Turbulent Shear Flow* (Cambridge U.P., New York, 1976).

[13]See Ref. 10 for an alternative view.

[14]R. H. Kraichnan, Adv. Math. 16, 305 (1975). R. H. Kraichnan, Phys. Fluids 7, 1723 (1964).

[15]For a similar calculation see T. Nakano, Ann. Phys. (N.Y.) 73, 326 (1972).

[16]To verify the correctness of our qualitative arguments regarding $\vec{V}_{l-1}\cdot\nabla\vec{V}_{l-1}$ we included it rather approximately in our program and reran for $\gamma=1.1$ and 1.3 and a self-consistent value of $\langle\eta_3\rangle$. No attempt was made to determine the best value of γ or include the companion term, $\vec{V}_l\cdot\nabla\vec{V}_{l+1}+\vec{V}_{l+1}\cdot\nabla\vec{V}_l$, in $d\vec{V}_l/dt$. The dissipation rate ϵ_l includes $\int_l V_l^{\alpha}\vec{V}_{l-1}\cdot\nabla\vec{V}_{l-1}^{\alpha}$ in addition to Eq. (5.3b), and η_l is again chosen to conserve energy. Somewhat surprisingly, the additional term in ϵ_l proved to be nearly always positive. For the same rate of energy input into the first shell, E_1 decreased by 30% implying the cascade has become more efficient. The Kolmogorov constant decreased from 3.5 to 2.5. For equivalent values of E_1, the cascade that included $\vec{V}_{l-1}\cdot\nabla\vec{V}_{l-1}$ dissipated 40% more energy/time. The variance of ϵ in corresponding shells decreased by a factor of 5–7 yet $\mu\sim0.8$–0.9 for $\gamma=1.3$; $\mu\sim0.6$ for $\gamma=1.1$ and ζ and δ were approximately zero.

[17]Cascade models with one mode per shell have been constructed by a number of authors. The model in (5.8) was first proposed by Oboukhov. If the mean-field value of $\vec{V}_{l-1}\cdot\nabla\vec{V}_{l-1}$ is included in (5.8) with a sign that augments the energy transfer and sufficient magnitude, the equations relax to Kolmogorov's 1941 theory. See V. N. Desnyansky and E. A. Novikov, Sov. J. Appl. Mech. (PMM) 38, 507 (1974) and T. Bell and M. Nelkin (unpublished).

[18]Experimental values of C_K range from 1.5 to 3.0. See Ref. 15.

[19]U. Schumann, J. Comput. Phys. 18, 376 (1975).

[20]J. W. Deardorff, J. Fluid Mech. 41, 453 (1970).

[21]A. Galilean transformation was implicitly made in treating the coupling to larger scales in Ref. 15.

[22]S. Orszag, J. Fluid Mech. 41, 363 (1970).